Accessing the developing CNS:
Advancing AAV-Mediated Prenatal Gene Editing in the Brain

Thesis by
Cameron Richard Jackson

In Partial Fulfillment of the Requirements for
the degree of
Doctor of Philosophy

CALIFORNIA INSTITUTE OF
TECHNOLOGY
Pasadena, California

2026
(Defended April 29, 2026)

Cameron Richard Jackson

ORCID: 0009-0008-7212-616X

Acknowledgements

To any young scientist reading this, I hope you enjoy the journey and live it to the fullest both inside and outside of the lab. Find the things that make you happy and chase them while you are young. Science is hard, and it looks you in the face every day and dares you to advance it in the wake of the thousands who have tried and failed before you. The best feelings I have had as a scientist have been the small advances toward solving a huge problem, so enjoy the little things. When you get good data, go home, and ride that feeling for the rest of the day before confirmatory experiments. Someone once told me that the purpose of a PhD is to understand how hard a problem can truly be. How amazing it is to be an investigator of the natural world, at the frontier and helm of seemingly infinite human knowledge.

I would like to thank the many amazing friends and mentors that have contributed to my life and research journey. You all have taken me from a young student who was enthralled by physical sciences and biology since childhood and refined me into a capable scientist. For these things I cannot thank you all enough. Science has always been my true and first love, and graduate school has been the highlight of my life because I have the opportunity to explore the natural world and life with virtually no boundaries, an experience of a lifetime.

First and foremost, I would like to thank my PI, Viviana Gradinaru. Even before I got into Caltech, Viviana had my back! She has given me the freedom and privilege to draft my own scientific journey and research. She has taken many, many, chances on me as a young student, and I am very grateful for the opportunities. I will always look to you as an example of what it means to be a great leader. I would also like to thank my committee for their insights and suggestions throughout my PhD; Marrianne Bronner, Carlos Lois, and Henry Lester. Marianne, you allowed me to rotate in your lab where I gained some amazing injection techniques in the chick embryo neural tube, these skills would go on to outline my thesis work and advance previous IUGT efforts in mammals. Henry and Carlos, I have had the privilege to teach with both of you and continue to be amazed by the wealth of knowledge between you both. You keep new students excited about the brain and inspire them (and me) to push the technological barriers for a deeper understanding.

I also want to thank my undergraduate mentor, Dr. Ketema Paul at UCLA. You have inspired me as a person, a researcher, and a social justice advocate. Thank you for your unwavering support and career discussions and guidance. You gave me my first true role as a scientist, and I hope to give many other young black scientists the same opportunities. Thanks for taking a chance on me and believing in me as a person and student.

I have been very fortunate to have been mentored by many amazing scientists in the Gradinaru Lab. Notably, I want to thank Gerry and Mate; the way you both design and execute your science is more than logic, protocols, and intuition – its art. And it's beautiful. It has been a pleasure to work with you both to gain design and technical skills in the lab. Mate, the times we spent late in

lab finding the vitelline vein will always be my fondest memories of graduate school, for a brief moment we were on the forefront of discovery and what was capable in science, a feeling I will strive to recreate in my research career. I also want to thank alumni who have contributed greatly to my learning and research, Xinhong Chen, David Goertsen, Miggy Chuapoco, and Min Jee Jang. Thank you to my peers in the lab, and supporting staff: Seongmin Jang, Changfan Lin, Sayan Dutta, Jonathan Hoang, Yujie Fan, Xuanjia Ye, Yeji Kim, Rana Eser, Amanda Wu, Ann Popovici, Catherine Oikonomou, Pat Anguiano, Elisha Mackey, Tim Shay, YP Lei, Fiona Ristic. Also, thank you to the three graduate students in my cohort, Karan Mahe, Alex Chung, and Tyler Brittain. We have grown so much together, and I look forward to your future endeavors, I know you all will do amazing things beyond graduate school.

I want to thank my family for their support throughout my life and graduate school. My mother Rosiland, my uncle James, my granny Laletha, and my late father, Richard. You all have given me such a strong love for knowledge since I was a child. Thank you for satiating my curiosities. Also, my sisters; Caira, Carrie, and Sage – you all are a very strong force in my life and inspire me to succeed. Especially Carrie, you have been my best friend for as long as I can remember and supported me in more ways than you realize.

To my amazing friends, you all are a light in my life and inspire me to be a better person. Thank you for all of your support and love. We have traveled the world together and made memories that will last a lifetime! Notably, thank you to Francisco and Louie – you guys are like the brothers I never had, thank you for being true friends I can always count on.

I dedicate my thesis work and the effort that has gone into this project to my future wife, children, and grandchildren. You are the source of any ambitions, and I hope some of my work will make a positive impact on your lives. I hope this PhD is representative of what life can be, regardless of what you come from, and regardless of how the world may treat you – hard work will always pay off, and you can accomplish great things.

Abstract

Targeted gene delivery to defined neural populations is a central challenge in neuroscience and a major barrier to gene therapy for neurodevelopmental and congenital disorders. In the developing central nervous system, this is further complicated by dynamic changes in accessibility, vector tropism, and cellular composition across developmental stages. This thesis develops new approaches for systemic prenatal CNS access, capsid engineering, and in utero genome editing in the embryonic brain.

We introduce UseqFISH, a spatial transcriptomic platform that enables high-sensitivity, multiplexed detection of endogenous transcripts, and barcoded viral genomes in intact tissue at single-cell resolution. This allows quantitative in situ mapping of AAV tropism and scalable evaluation of viral libraries in embryonic contexts. Using new and existing techniques, we characterize systemic AAV biodistribution across development and show that adult brain-biased serotypes do not maintain specificity in late-mid gestation embryos. We engineer modified capsids, including “null” scaffolds with reduced native tropism, which can be reprogrammed via targeting motifs. High-throughput barcoded in vivo selection identifies sequence features associated with improved CNS enrichment during embryogenesis.

To expand access to midgestational delivery, we develop a surgical method enabling systemic AAV administration at embryonic day 12.5 via uterine microdissection of the vitelline circulation, achieving widespread and viable transduction through gestational development. Finally, we established an in utero genome editing platform using AAV-mediated CRISPR and homology-directed repair. We demonstrate efficient gene disruption, epitope tagging, and precise genome modification, including endogenous tagging and introduction of disease-associated alleles across cortical cell types, enabling modeling of neurodevelopmental phenotypes.

Together, this work provides a framework for engineering AAV-based gene delivery and genome editing in the developing CNS, advancing tools for studying brain development, modeling disease, and enabling early therapeutic strategies.

Published Content and Contributions

1. *Defining a Midgestational Window for In Utero Genome Editing of the Fetal Murine Cortex.*
   Cameron R. Jackson, Máté Borsos, Nathan Appling, Carrie R. Jackson, Gerard M. Coughlin, Viviana Gradinaru. BioRxiv (2026) DOI:10.64898/2026.04.28.721509

   Contributions: Conceived the study, oversaw the project direction, wrote the manuscript, generated the figures with input from all authors, carried out the majority of experiments, performed data collection and analyses, conceptualized and optimized microinjection techniques.

2. *Spatial transcriptomics for profiling the tropism of viral vectors in tissues.*
   Min J. Jang, Gerard M. Coughlin, **Cameron R. Jackson**, Xinhong Chen, Miguel R. Chuapoco, Julia L. Vendemiatti, Alexander Z. Wang & Viviana Gradinaru. Nature Biotechnology 41, 1272–1286 (2023). DOI: 10.1038/s41587-022-01648-w

   Contributions: Performed experiments for *Hexb* probe validation and assisted with USeqFISH profiling data collection

3. *Spatial genomics of AAV vectors reveals mechanism of transcriptional crosstalk that enables targeted delivery of large genetic cargo.*
   Gerard M. Coughlin, Máté Borsos, Bre'Anna H. Barcelona, Nathan Appling, Acacia M. H. Mayfield, Elisha D. Mackey, Rana A. Eser, **Cameron R. Jackson**, Xinhong Chen, Sripriya Ravindra Kumar & Viviana Gradinaru. Nature Biotechnology 44, 133–145 (2025). DOI: 10.1038/s41587-025-02565-4

   Contributions: Created constructs used in spot size assessment.

4. *Schwann cell precursors represent a neural crest-like state with biased multipotency.*
   Kastriti, M.E., Faure, L., Von Ahsen, D., Bouderlique, T.G., Boström, J., Solovieva, T., **Jackson, C**., Bronner, M., Meijer, D., Hadjab, S., Lallemend, F., Erickson, A., Kaucka, M., Dyachuk, V., Perlmann, T., Lahti, L., Krivanek, J., Brunet, J.-F., Fried, K., Adameyko, I. EMBO Journal 41, e108780 (2022). DOI: 10.15252/embj.2021108780

   Contributions: Neural tube injections, formal analysis, investigation, and visualization.

Table of Contents

Chapter I:

Introduction

1.1 AAV vectors for gene therapy

Adeno-associated viruses (AAVs) have become one of the leading platforms for in vivo gene delivery due to their favorable safety profile, low immunogenicity, and ability to support long-term transgene expression [R1]. As non-pathogenic viruses with a relatively simple genome, AAVs can be engineered to carry therapeutic or experimental payloads while maintaining efficient transduction across a range of tissues. Different naturally occurring and engineered capsid variants exhibit distinct tropisms, enabling selective targeting of the central nervous system, peripheral organs, and other specialized cell populations. These properties have made AAVs a central tool in both basic neuroscience research and the development of gene therapies for a growing number of genetic diseases [R2, R3].

Despite these advantages, precise control over cell-type specificity remains a major challenge. AAV tropism is influenced by multiple factors, including capsid composition, route of administration, cargo regulatory elements, and host biology, and even well-characterized variants often show broad or context-dependent expression patterns [R4]. To improve targeting precision, extensive efforts have focused on capsid engineering and library-based screening approaches that generate large pools of candidate variants.

1.2 Mapping vector delivery in the CNS with spatial transcriptomics

Targeted gene delivery to defined cell types is fundamental to both neuroscience and gene therapy, enabling controlled expression of reporters, sensors, effectors, and genome editors. While advances in viral engineering, particularly with AAVs, have expanded targeting capabilities, a general strategy for achieving high specificity across the full diversity of molecularly distinct cell types remains unresolved [R1, R3]. This challenge is especially critical in therapeutic settings, where off-target expression can compromise safety [R5, R6]. At the same time, the rapid growth of engineered viral libraries has outpaced methods for characterizing their tropism, as existing approaches often lack the sensitivity, spatial context, or single-cell resolution needed for comprehensive in vivo analysis.

To address these limitations, we developed UseqFISH, a spatial transcriptomic method for high-sensitivity, multiplexed detection of RNA directly in intact tissue. The approach integrates padlock probe hybridization with rolling circle amplification and hybridization chain reaction to generate strong localized signals, enabling robust detection with relatively few probes per target. This improves signal-to-noise while preserving spatial resolution and allows for reliable measurement of low-abundance transcripts and short barcoded sequences. As a result, UseqFISH supports

simultaneous readout of endogenous gene expression and viral identity within the same cellular context.

By incorporating sequential and combinatorial barcoding strategies, the method achieves scalable multiplexing without increasing barcode length, making it well suited for AAV systems with limited packaging capacity. This framework exponentially increases the current UseqFISH target capacity, enabling in situ profiling of large pooled viral libraries, and allowing direct comparison of variants within the same tissue environment. Consequently, UseqFISH v2 provides a platform for mapping AAV tropism at single-cell resolution while maintaining spatial organization, bridging the gap between high-throughput viral engineering and functional interpretation.

1.3 AAV's for in utero gene therapy and limitations

Recombinant adeno-associated viruses (AAVs) have emerged as leading vehicles for *in utero* gene therapy due to their favorable safety profile, low immunogenicity, and customizable genetic cargo [14, 15]. AAVs can deliver transgenes, regulatory elements, and gene editing machinery with minimal unintended genomic integration [16, 17]. Importantly, single-dose AAV administration is well tolerated by the fetal immune system, and the small size of the fetus enables efficient systemic delivery using substantially lower vector doses than those required in postnatal or adult settings [18]. Despite these advantages, significant challenges remain. Efficient and selective delivery to the developing CNS remains difficult, and systemic administration of AAVs often results in substantial off-target liver transduction, limiting therapeutic efficacy and raising safety concerns [14, 19].

To date, most AAV-based prenatal therapies have relied on gene replacement strategies, in which therapeutic efficacy depends directly on transduction efficiency in target cells [20]. In the developing fetus, however, rapid cell division leads to dilution of episomal viral genomes, leading to diminished transgene expression [21, 22]. In contrast, genome editing offers the potential for permanent genetic modification, particularly when targeting proliferative progenitor populations early in development [23, 24, 25]. CRISPR/Cas9-based *in utero* genome editing has been demonstrated in the fetal mouse, but reported editing efficiencies in the brain remain low when editors are delivered systemically using AAV9 at or after embryonic day 14.5 (E14.5) [26]. As in juvenile and adult animals, the liver captures a substantial fraction of systemically delivered virus at these stages, limiting CNS access [27]. These observations suggest that developmental timing, rather than vector choice alone, may be a critical determinant of successful prenatal genome editing in the brain.

1.4 Advancing in utero gene editing in the CNS

Congenital disorders comprise a diverse group of conditions that arise during fetal development or at birth, leading to structural or functional abnormalities with lifelong consequences [1]. Among these, disorders affecting the central nervous system (CNS) are particularly devastating, as the

brain undergoes rapid and highly coordinated development beginning shortly after fertilization and continuing into adolescence and adulthood [2, 3, 4]. The brain grows more rapidly *in utero* than at any other stage of life, rendering early neurodevelopment uniquely susceptible to genetic and environmental perturbations [5,6]. CNS abnormalities occur in nearly 1 in 100 live births, with malformations of the cerebral cortex representing a major subset of these conditions [7, 8].

Malformations of cortical development (MCDs) frequently arise from genetic variants affecting key neurodevelopmental genes [9]. A 2024 retrospective study of 32 prenatally diagnosed MCD cases identified single nucleotide or copy number variants in 22 affected fetuses, revealing the predominance of discrete genetic lesions in these disorders [10]. Notably, 31 of the 32 pregnancies were terminated, highlighting the absence of effective prenatal treatment options and the limited ability to predict postnatal outcomes. These findings underscore the urgent need for strategies that enable both functional modeling and therapeutic intervention during fetal brain development.

Prenatal gene therapy offers a compelling opportunity to intervene before irreversible neurodevelopmental defects are established [11]. Treating the fetus at early developmental stages has shown therapeutic potential across multiple mammalian systems [12]. Systemic delivery approaches have successfully accessed diverse fetal organs and cell types in both mouse and human, including in recent clinical studies in which enzyme replacement therapies delivered via the umbilical vein enabled prenatal treatment of an otherwise lethal lysosomal storage disorder [13]. These examples illustrate the feasibility and potential impact of treating disease at its developmental origin rather than after birth.

Midgestational stages, between E11 and E15 in the mouse, encompass critical transitions in both hepatic and cortical development. During this window, the fetal liver gains functionality, and neural progenitor populations undergo rapid expansion and migration [28, 29]. Early midgestation (E10-E12.5) marks the decline of dominating stemness-associated gene expression in the cortical neuroepithelium, followed by increasing neuronal differentiation, deep layer cortical lamination, and fate specification [30, 31, 32]. Access to the embryo during this period is therefore particularly attractive for genetic intervention targeting cortical progenitors. However, systemic AAV delivery at these stages is technically constrained. Placenta-crossing vectors capable of achieving reliable fetal CNS delivery have not yet been developed, rendering maternal injection ineffective [33]. Direct injection into the embryonic circulation circumvents this limitation but has historically been restricted to later gestational stages, as uterine opacity and tissue density prior to E14 prevent visualization of the murine vitelline vein using standard techniques [34].

Advancing safe and effective *in utero* genome editing in the developing cortex has broad implications for both therapy and disease modeling. From a translational perspective, editing the fetal genome of wild-type mice would enable rapid functional evaluation of pathogenic variants identified during prenatal screening, providing critical insight into disease severity and potential postnatal outcomes. Further, efficient genome editing in the embryonic cortex would enable rapid

modelling of rare human neurodevelopmental disorders in mice within weeks. Coupling refined surgical access with modern genome editing tools thus offers a powerful framework for investigating cortical development, modeling congenital disorders, and exploring early therapeutic intervention strategies. Toward this goal, we integrate uterine microdissection–based vascular access with systemic AAV delivery to define a permissive early midgestational window for prenatal gene delivery and genome editing in the mouse cortex.

Chapter II:

Spatial Transcriptomics for Enhanced AAV Tropism Profiling

2.1 Summary

Targeted gene delivery to specific cell types is central to both neuroscience and gene therapy. It enables precise expression of reporters, sensors, effectors, and genome editors in defined cellular populations, which is essential for dissecting circuit function and developing therapeutic strategies. Despite major advances in viral engineering and targeting approaches, we still lack a general solution for accessing the full diversity of molecularly distinct cell types with high specificity. This limitation is especially important in therapeutic contexts, where off-target expression can directly impact safety.

Here, we developed and applied UseqFISH, a spatial transcriptomic approach designed for high-sensitivity, multiplexed readout of endogenous genes and barcoded viral transcripts directly in intact tissue. The goal is to enable single-cell resolution mapping of AAV tropism in situ at a scale compatible with modern viral libraries.

2.2 Introduction

AAVs are widely used for in vivo gene delivery due to their relatively low immunogenicity, stable expression, and broad range of natural and engineered tropisms. Over the past decade, capsid engineering efforts (including directed evolution and rational design) have produced variants with improved targeting across the central and peripheral nervous systems, as well as peripheral tissues such as muscle and vasculature, in both rodent and non-human primate models. However, the ability to characterize AAV specificity has not kept pace with the scale of library generation. While high-throughput screening approaches can evaluate large numbers of variants, downstream validation of tropism is often limited to low-throughput assays that lack single-cell resolution and spatial context. This creates a bottleneck between discovery and functional interpretation.

2.3 UseqFISH for enhanced tropism profiling.

To address this, we developed UseqFISH (Fig. 1), a spatial transcriptomic method optimized for sensitive and multiplexed RNA detection in intact tissue. UseqFISH combines padlock probe hybridization with rolling circle amplification (RCA) and hybridization chain reaction (HCR) to generate strong, localized signal at the site of each transcript. This amplification strategy enables reliable detection using only a small number of probes per target gene, improving signal-to-noise while maintaining spatial resolution.

A key advantage of this approach is that it enables detection of low-abundance transcripts and compact barcoded sequences, making it compatible with AAV systems where barcode length is

constrained. In practice, this allows simultaneous readout of endogenous gene expression and viral identity within the same cellular context.

Existing spatial transcriptomic methods face several limitations when applied to viral tropism mapping. Many approaches rely on multi-probe targeting schemes that require relatively long transcript regions to achieve specificity, which is incompatible with the limited packaging capacity of AAV vectors (~4.7 kb total). Systemic AAV delivery further complicates detection because individual variants often have low copy numbers per cell. As a result, sensitivity becomes a major limiting factor. Bulk approaches such as qPCR or sequencing are useful for narrowing viral libraries but lack spatial and single-cell resolution. Immunohistochemistry provides spatial context but is restricted by antibody availability and limited multiplexing. Single-cell RNA sequencing improves resolution but loses spatial organization entirely. Together, these limitations highlight the need for a method that combines sensitivity, spatial resolution, and compatibility with short barcodes.

UseqFISH addresses these constraints primarily by increasing detection sensitivity, which reduces the number of probes required per transcript and enables shorter, AAV-compatible barcodes. We further extend this framework using sequential and combinatorial barcoding strategies. In this design, padlock probes contain multiple reader binding sites that can be independently interrogated across imaging cycles (Fig. 3). Each site is decoded through orthogonal fluorescent readouts, enabling combinatorial expansion of detectable targets. This structure increases effective multiplexing capacity without increasing barcode length. Importantly, even in single-round experiments, multiple reader probes can be detected cleanly, supporting scalability to sequential imaging workflows.

2.4 AAV tropism mapping using multiplexed UseqFISH (v2).

We applied multiplexed UseqFISH to detect endogenous cell markers directly in intact brain tissue (Fig. 4). Using sequential barcoding across multiple imaging rounds, we uniquely identified multiple transcripts within a subpopulation of cortical cells. Each gene is assigned a combinatorial signature across imaging cycles, enabling unambiguous identification at single-cell resolution. This approach allows direct linking of viral identity to host cell transcriptional state while preserving spatial context. As a result, we can resolve how distinct AAV variants distribute across cell types and brain regions within the same experiment.

This framework enables in situ analysis of pooled AAV libraries rather than one-by-one validation. Each variant is encoded with a short barcode that can be read out alongside endogenous markers. Because measurements are made in the same tissue context, variants can be directly compared under identical biological conditions. This allows not only quantification of overall transduction efficiency, but also resolution of subtle differences in cell-type specificity and regional bias that are often missed in bulk analyses.

Beyond capsids, UseqFISH can also be applied to regulatory elements embedded in AAV genomes. This includes promoter variants and microRNA target sites that influence expression across cell types. By encoding these elements as part of the barcode design, their effects can be directly measured in situ across heterogeneous tissue environments. This expands the system from capsid screening to a more general platform for evaluating gene regulation strategies in spatial context.

2.5 Methods

Reagents

All experiments were performed using standard molecular biology and imaging reagents, including buffers for nucleic acid hybridization (SSC, formamide), enzymatic reactions (T4 ligase, Phi29 polymerase, dNTPs), and signal amplification (HCR hairpins). Additional reagents included paraformaldehyde (PFA) for fixation, detergents (Tween-20, SDS) for permeabilization and clearing, and hydrogel components (acrylamide, bisacrylamide, APS, TEMED) for sample embedding. RNase inhibitors and blocking reagents (RVC, SUPERase, salmon sperm DNA, BSA) were used to preserve RNA integrity and reduce nonspecific binding.

Cell Culture and Transfection

HEK293T cells were maintained under standard conditions and transfected with AAV genome plasmids using polyethylenimine (PEI). Cells were fixed 72 hours post-transfection in 4% PFA and stored in ethanol prior to downstream processing. For single-probe amplification experiments, NIH3T3 cells were cultured in DMEM supplemented with fetal bovine serum. Cells were plated at low density on poly-D-lysine and laminin-coated surfaces, fixed within 12–24 hours, and stored in ethanol until use.

Tissue Preparation

Mouse and primate brain tissues were sectioned using a vibratome (50–75 μm thickness), followed by post-fixation in 4% PFA. Samples were dehydrated in ethanol and later rehydrated through graded ethanol washes prior to UseqFISH processing. For thick tissue imaging, samples were embedded in a hydrogel matrix and cleared using SDS-based protocols to improve probe penetration and optical accessibility.

UseqFISH Workflow

UseqFISH was performed through sequential steps of probe hybridization, ligation, amplification, and imaging. Briefly, target-specific padlock probes were hybridized to RNA transcripts in a formamide-based buffer. Following hybridization, probes were ligated to form circular templates. Rolling circle amplification (RCA) was then carried out using Phi29 polymerase to generate

localized DNA amplicons. These amplicons were subsequently labeled using hybridization chain reaction (HCR), producing amplified fluorescent signal at each target site.

To stabilize signal and maintain spatial fidelity, samples were functionalized and embedded in a polyacrylamide hydrogel prior to imaging. For tissue samples, additional clearing and enzymatic treatments were incorporated to improve probe accessibility and signal consistency.

Sequential Imaging and Signal Reset

Multiplexed detection was achieved through sequential rounds of labeling and imaging. After each imaging cycle, fluorescent signal was removed using a combination of strand displacement and high-formamide washes, allowing new probe sets to be applied. Custom-designed toehold-mediated displacement oligonucleotides were used to selectively remove HCR assemblies, enabling iterative readout of multiple targets within the same sample. Nuclear staining and cytosolic labeling were included in final imaging rounds for cell segmentation and spatial reference.

Imaging and Instrumentation

Fluorescence imaging was performed using widefield and confocal microscopy systems. High-resolution volumetric imaging was conducted using spinning disk confocal microscopy with automated fluidics control to enable sequential reagent exchange. Custom scripts were used to coordinate imaging and fluid handling, allowing reproducible multi-round acquisition across large tissue volumes. Imaging resolution was optimized to achieve subcellular localization of transcript signals.

Barcode and Probe Design

Barcodes and probe sequences were computationally designed to maximize hybridization efficiency and minimize cross-reactivity. Barcode sequences were constrained by GC content, melting temperature, and sequence complexity, and were screened against transcriptome databases to avoid off-target binding. Padlock probes and primers targeting endogenous genes were designed using custom scripts incorporating sequence filtering and alignment tools. Probe sets were optimized to maintain specificity while minimizing the number of required binding sites per transcript.

AAV Library Construction and Production

Barcoded AAV genome plasmids were generated by inserting synthetic barcode sequences into a reporter backbone under a constitutive promoter. Viral particles were produced in HEK293T cells via triple transfection and purified using iodixanol gradient ultracentrifugation. Viral titers were quantified using qPCR or digital droplet PCR, and individual variants were pooled at defined ratios prior to in vivo administration.

In Vivo Delivery and Tissue Collection

AAV libraries were delivered systemically via intravenous injection in mice and non-human primates. After an appropriate expression period, animals were perfused, and brains were harvested and fixed. Tissue samples were sectioned and processed for UseqFISH as described above. All animal procedures were performed in accordance with institutional guidelines.

Validation with Immunohistochemistry and FISH

Selected experiments were validated using immunohistochemistry and conventional fluorescence in situ hybridization (FISH). Antibody labeling was used to identify major cell types, while smFISH and HCR-based methods were used to benchmark transcript detection sensitivity and specificity.

2.6 Figures

Figure 1: UseqFISH for spatial transcriptomic profiling

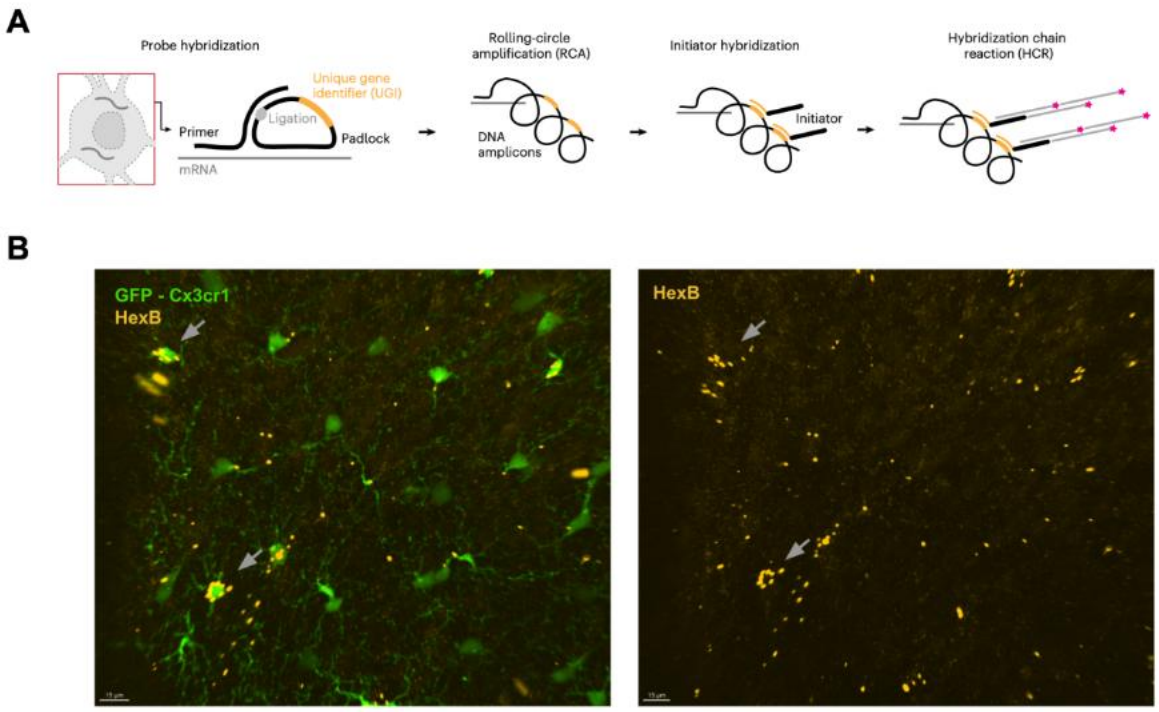

Figure 1. UseqFISH enables spatial transcriptomic profiling of endogenous mRNA in tissue.

(A) Schematic of the UseqFISH workflow, adapted from Jang et al. 2023. Multicomponent and padlock probes hybridize to the target transcript, followed by ligation, rolling circle amplification (RCA), and hybridization chain reaction (HCR) for signal amplification. (B) Detection of endogenous HexB mRNA in mouse tissue from a Cx3cr1-GFP mouse line. Colocalization of GFP and HexB signal confirms successful UseqFISH labeling.

Figure 2: Reduced barcode length for 7-mer detection with UseqFISH

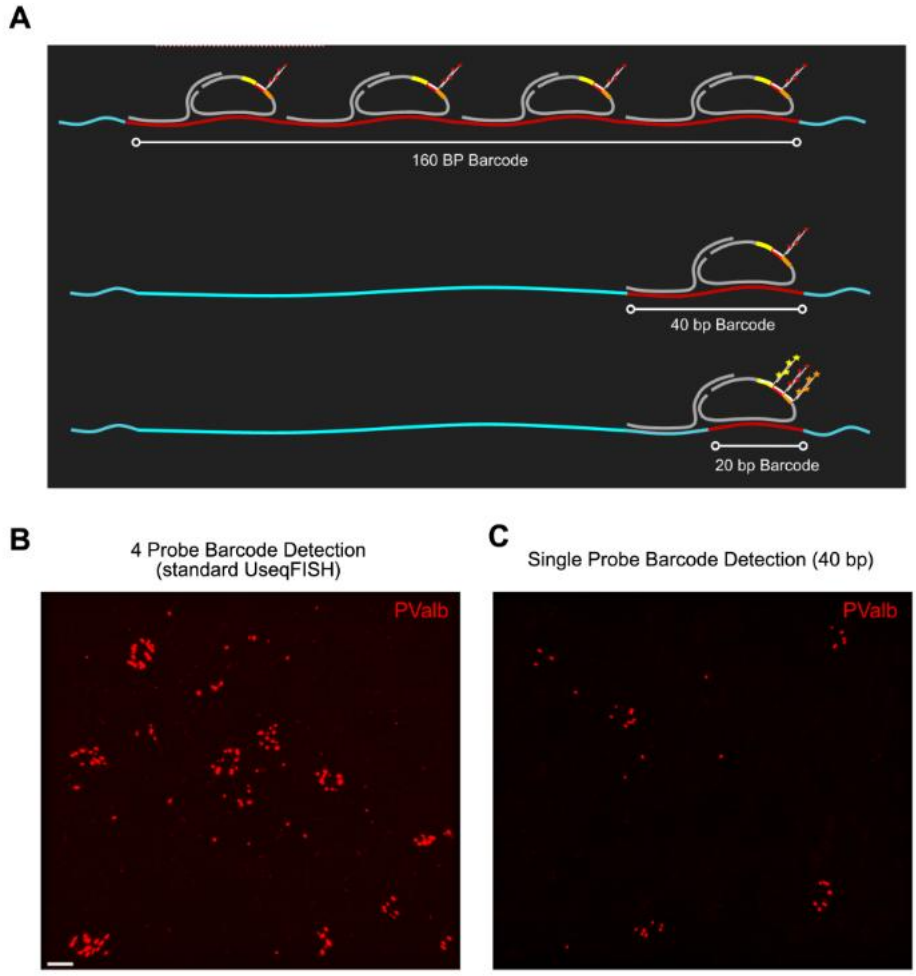

Figure 2. Reduced barcode length decreases detection efficiency in UseqFISH.

(A) Schematic illustrating barcode design variants with decreasing target length and probe complexity: a 160 nt barcode detected using four complementary probes, a 40 nt barcode detected with a single fully complementary probe, and a 20 nt barcode with complementarity restricted to the padlock probe region. (B) UseqFISH signal from the standard configuration (160 nt barcode, four probes) showing robust detection with high spot density. (C) UseqFISH signal from the same tissue and imaging conditions as in (B), but using a single-probe 40 nt barcode, demonstrating reduced spot number and decreased detection efficiency of target barcodes.

Figure 3: Multiplexed sequential barcoding design increases UseqFISH readout capacity.

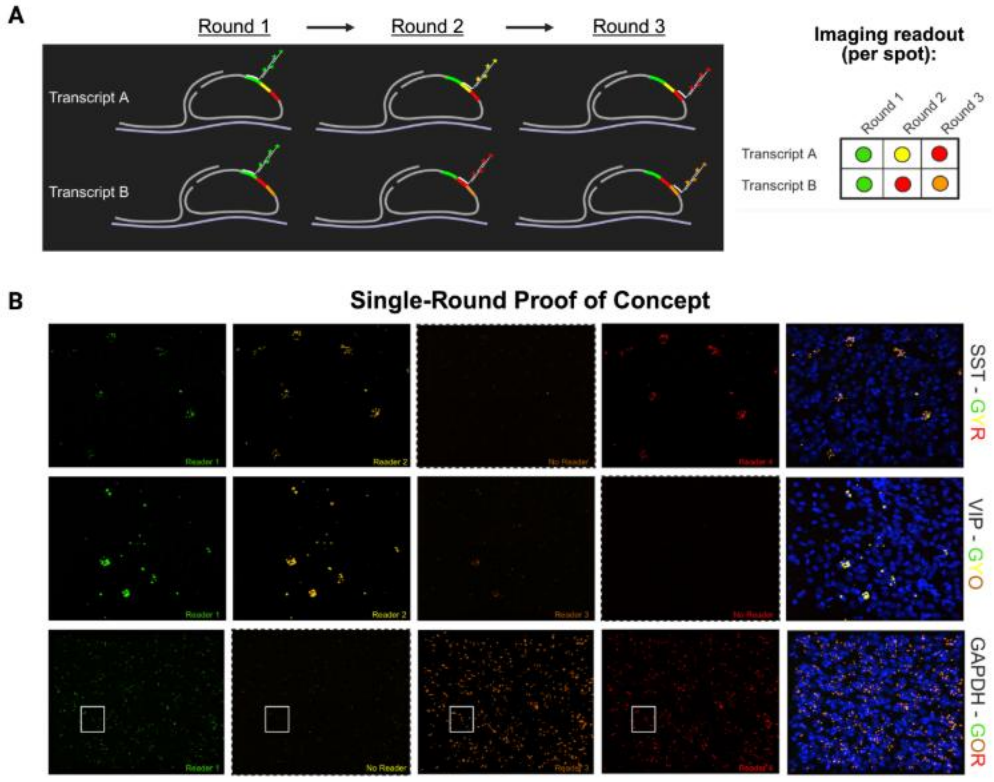

Figure 3. Multiplexed sequential barcoding expands UseqFISH readout capacity.

(A) Schematic of a color-barcoded UseqFISH design utilizing an extended padlock probe containing three distinct reader binding sites, each enabling independent hybridization chain reaction (HCR) amplification. This architecture allows combinatorial, multiplexed imaging across transcripts, illustrated by example readouts for Transcript A and Transcript B (right). (B) Single-round proof-of-concept of the UseqFISH barcoding scheme, in which multiple reader probes were applied simultaneously. Detection of signal from each reader demonstrates that all padlock-encoded sites are compatible with multiplexed color barcoding within a single imaging round, supporting their use across multiple sequential imaging rounds.

Figure 4: Multi-round sequencing by competition enables unique gene identification across imaging rounds.

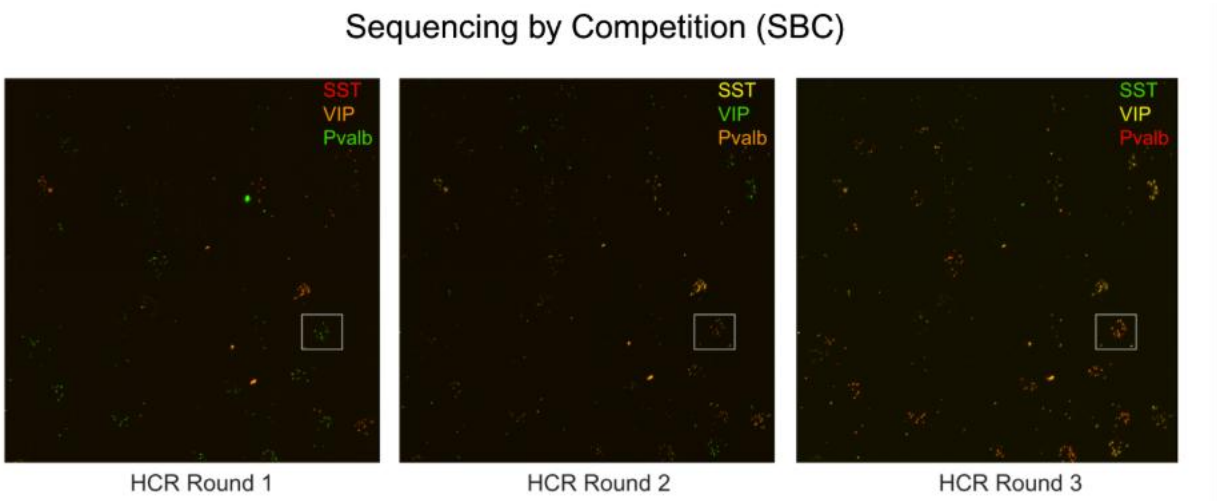

Figure 4. Multi-round sequencing by competition enables unique gene identification across imaging rounds. Representative field of view (FOV) showing color-barcoded UseqFISH signal across three sequential imaging rounds for three distinct endogenous genes. Sequential rounds of reader hybridization and signal acquisition generate unique combinatorial barcodes for each transcript, enabling gene identification within a single sample.

2.7 Discussion

UseqFISH enables direct spatial mapping of viral delivery at single-cell resolution, linking viral identity, host cell type, and tissue context within a unified experimental framework. The central advance is the coupling of high-sensitivity RNA detection with compact, AAV-compatible barcodes and multiplexed sequential imaging. Together, these features make it possible to reduce barcode length to levels that fit within AAV packaging constraints while still preserving enough information content for library-scale profiling in intact tissue. This closes a key gap between large-scale viral screening and high-resolution validation, where previously these steps were largely disconnected.

At a conceptual level, this shifts how viral screening is performed. Instead of a two-stage workflow, first screen a library in bulk or pooled format, then validate candidates with low-throughput histology, the readout becomes inherently spatial and single-step. Viral tropism is no longer inferred indirectly from dissociated tissue or population averages, but directly measured in situ while preserving both cellular identity and anatomical context. This makes tropism mapping fundamentally a spatial measurement problem rather than a downstream validation step.

However, several important limitations remain. First, sequential imaging depends critically on the ability to efficiently remove and re-bind reader probes across rounds. In the current

implementation, reader binding dynamics are not yet fully optimized. Incomplete dissociation between cycles can lead to residual signal carryover, reduced contrast, and compression of dynamic range across rounds. This becomes increasingly important as the number of imaging cycles increases, since small inefficiencies compound over repeated rounds. Improving hybridization stringency, wash conditions, and probe chemistry will be necessary to ensure clean cycle resetting and robust decoding performance at higher multiplexing depths.

Second, reducing barcode length-while necessary for compatibility with AAV genome constraints-introduces a measurable tradeoff in detection efficiency. As shown in Fig. 2, shorter barcode regions lead to reduced spot recovery compared to longer, multi-probe designs. This is likely due to a combination of reduced hybridization surface area, increased sensitivity to local sequence context, and stochastic loss of binding events when probe numbers are minimized. While UseqFISH amplification partially compensates for this loss, detection efficiency is not fully invariant to barcode length. Importantly, this limitation is not purely methodological but also design-dependent. One path forward is to treat barcode architecture as a co-optimized component of the viral library itself. Instead of adapting UseqFISH to arbitrary sequences, AAV libraries can be engineered to include dedicated UseqFISH-compatible barcode regions that are optimized for probe binding, amplification efficiency, and minimal secondary structure. This co-design strategy between viral engineering and spatial readout is likely essential for maximizing performance in large-scale screens.

Finally, multiplexing capacity depends strongly on the encoding strategy. In the current non-combinatorial implementation, the number of distinguishable targets scales approximately as $4n$, where n corresponds to the number of orthogonal imaging or HCR rounds (typically fewer than ~10 in practice due to imaging time and tissue stability constraints). While this linear scaling already enables substantial multiplexing, it remains fundamentally limited when considering large viral libraries or highly complex regulatory screens.

In contrast, the multiplexed UseqFISH v2 architecture introduces combinatorial encoding through multiple reader binding sites per padlock probe. In this framework, each target is defined not by a single readout event but by a combination of signals across multiple sites and rounds. This shifts the scaling behavior to approximately 4^n, where each additional round exponentially increases the number of possible unique barcodes. Even with modest values of n, this exponential expansion produces a dramatic increase in theoretical target capacity, making it feasible to encode large AAV libraries, regulatory element libraries, and potentially multi-layered perturbation systems within a single experiment.

Despite these constraints, UseqFISH v2 provides a scalable framework for in situ functional screening of viral vectors and regulatory elements. More broadly, it establishes a general approach for spatially resolved genetic screening, where delivery, expression, and cellular identity can all be measured simultaneously in intact tissue. In this framework, viral engineering and spatial

transcriptomics are no longer separate stages of experimentation but become tightly integrated components of a single measurement system.

Chapter III:

Surgical Innovation Toward E12.5 Systemic Access.

3.1 Summary

Efficient systemic delivery to the developing embryo during early-to-midgestation remains a major technical challenge. While vitelline vein injection enables robust delivery at later stages (>E14.5), earlier access has been limited by uterine opacity, restricting genetic manipulation during a critical window of cortical neurogenesis.

Here, we present a surgical framework that enables reproducible systemic delivery at E12.5 through uterine microdissection-based exposure of the vitelline circulation. This approach allows consistent intravascular access while preserving embryonic viability and supporting development to term. Using dextran dye and AAV delivery, we demonstrate rapid, widespread systemic distribution and functional transduction, including successful recombination in reporter embryos. Together, this work extends the window for *in utero* systemic delivery into early midgestation, overcoming a technical limitation to provide a platform for developmental studies, disease modeling, and prenatal genome editing.

3.2 Introduction

Midgestational stages, between E11 and E15 in the mouse, encompass critical transitions in both hepatic and cortical development. During this window, the fetal liver transitions from a primarily hematopoietic organ to one acquiring metabolic functionality, while neural progenitor populations in the cortex undergo rapid expansion, lineage commitment, and migration. Early midgestation (E10-E12.5) marks a pivotal shift in the cortical neuroepithelium, characterized by the downregulation of stemness-associated transcriptional programs and the onset of neuronal differentiation, followed by deep-layer neuron formation and laminar organization. These tightly coordinated processes define a narrow temporal window in which genetic perturbation can have profound and lasting effects on cortical architecture and function.

Access to the embryo during this period is therefore particularly attractive for genetic intervention targeting cortical progenitors. However, systemic adeno-associated virus (AAV) delivery at these stages remains technically constrained. Placenta-crossing vectors capable of achieving robust fetal central nervous system (CNS) transduction have not yet been realized, rendering maternal delivery ineffective for early to midgestational targeting. Direct intravascular injection circumvents placental barriers but has historically been limited to later gestational stages (≥E14), where uterine translucency permits visualization of the vitelline vasculature. Prior to this stage, uterine opacity obscures vascular landmarks, preventing reliable access to the embryonic circulation.

In this chapter, we overcome this limitation by integrating uterine microdissection with optimized vitelline vein injection, enabling reproducible systemic delivery at E12.5. This approach expands the accessible window for prenatal gene delivery and provides a platform for efficient targeting of the developing cortex.

3.3 Building Upon Existing Frameworks for In Utero Systemic Delivery

Overcoming the technical barrier to early gestational vascular access unlocks a critical window for systemic delivery at the onset of cortical neurogenesis. Access at E12.5 enables perturbation of progenitor populations prior to extensive lineage diversification, allowing for more uniform targeting and reducing the mosaicism commonly observed with later-stage interventions. This is particularly important for applications requiring broad cellular coverage, such as genome editing or lineage tracing.

Existing approaches to *in utero* gene delivery have largely relied on either maternal administration of engineered viral vectors or direct embryonic injections at later gestational stages. While maternal delivery offers a non-invasive route, the absence of efficient placenta-transiting AAV capsids limits its utility for fetal CNS targeting. Conversely, direct intravascular injection, most commonly via the vitelline vein, provides robust systemic distribution but has traditionally been restricted to E14.5 and beyond due to visualization constraints. As a result, current methodologies are biased toward later developmental stages, after key neurogenic events have already been initiated.

The approach described here builds upon these frameworks by introducing uterine microdissection as a means to bypass technical limitations imposed by the early gestational uterus. By creating a localized uterine window, the vitelline vasculature can be directly visualized at E12.5 without compromising overall embryonic viability. When combined with optimized needle geometry and controlled microinjection parameters, this enables consistent intravascular access and efficient systemic delivery at earlier developmental time points than previously achievable.

From a translational perspective, extending systemic delivery into early midgestation provides a powerful platform for fetal genome editing and disease modeling. Editing the fetal genome in wild-type embryos could allow rapid functional interrogation of variants identified during human prenatal screening, enabling prospective assessment of disease phenotypes prior to birth. In parallel, early-stage delivery facilitates rapid generation of somatic models of neurodevelopmental disorders, significantly accelerating experimental timelines relative to traditional germline approaches.

Together, these advances position early midgestational systemic delivery as a versatile and scalable strategy for studying developmental processes, modeling human disease, and exploring the feasibility of prenatal therapeutic intervention

3.4 Methods

Timed Matings

Female mice were placed into cages with stud males during the dark (active) phase to maximize mating efficiency. The presence of a copulatory plug the following morning was taken as evidence of successful mating. Noon (12:00 PM) on the day of plug detection was designated as embryonic day 0.5 (E0.5), ensuring consistent developmental staging across experiments. Pregnant dams were monitored daily and maintained under standard housing conditions until the day of surgery.

Surgery and Injections

Pregnant dams were anesthetized using isoflurane delivered via a precision vaporizer (5% for induction, 1–2% for maintenance) and maintained on a heated surgical platform to preserve body temperature. Preoperative analgesia was administered subcutaneously, including ketoprofen (5 mg kg^{-1}) for anti-inflammatory effects and extended-release buprenorphine (3.25 mg kg^{-1}) for sustained analgesia. To maintain hydration and reduce surgical stress, 1 mL of sterile saline was delivered subcutaneously prior to incision.

The abdominal area was shaved and sterilized using alternating scrubs. For additional local anesthesia, one subcutaneous injection of bupivacaine was administered along the planned incision line. Throughout the procedure, anesthetic depth was continuously monitored via respiratory rate and pedal reflex.

Laparotomy and Uterine Window (E12.5)

A midline laparotomy (~2.5 cm) was performed to expose the uterine horns. Using sterile forceps, individual uterine horns were gently exteriorized and supported on sterile gauze pre-soaked in warm saline to prevent desiccation and maintain physiological conditions. Care was taken to minimize mechanical stress and preserve placental integrity.

At E12.5, visualization of the vitelline vasculature is hindered by uterine opacity. To overcome this, a targeted uterine microdissection was performed. Opposite the placental implantation site, identified by its characteristic shape and vascular density, and above regions containing clustered blood islands, the uterine wall was carefully thinned and dissected using fine forceps to create an approximately 3.5 mm “uterine window”. This window exposed the underlying yolk sac and vitelline vein while maintaining structural support from surrounding tissues. This approach enabled direct visualization of the vitelline vein on the yolk sac surface under a stereomicroscope, providing a stable and reproducible entry point for intravascular injection (Supplementary Video).

Needle Fabrication and Microinjection

Injection needles were fabricated from borosilicate glass capillary tubes (OD 1.00 mm) using a vertical puller to achieve a fine taper suitable for vascular access. Needles were subsequently trimmed using a microforge to produce a tip diameter of approximately 20 μm, balancing penetration efficiency with minimized vascular damage. A bevel angle of ~20° was applied using a microgrinder to facilitate smooth entry into the vessel lumen and reduce resistance during insertion. Concentrated AAV preparations or fluorophore-conjugated dextran dye were backfilled into the needles and mounted onto a precision microinjector. Under stereoscopic guidance, the needle was aligned parallel to the vitelline vein to minimize shear stress and reduce the likelihood of vessel rupture. The needle was advanced carefully until a brief “flash” of fetal red blood cells was observed within the needle tip, confirming successful intravascular placement.

Approximately 5 μL of solution was delivered via controlled pulse injection in the direction of blood flow to promote systemic distribution. Successful injections were typically characterized by rapid clearance of injected material into the circulation without local pooling. Following injection of 3-4 embryos per dam, the uterine horns were gently repositioned into the abdominal cavity. The peritoneal wall and skin were sutured in separate layers using absorbable sutures. Dams were allowed to recover on a heated pad and monitored postoperatively before being returned to their home cage. Embryos were harvested at defined time points (e.g., E18.5) or allowed to progress to birth for survival analysis.

3.6 Figures

Figure 1: E15.5 and E12.5 vitelline veins and access to fetal circulation from the yolk sac.

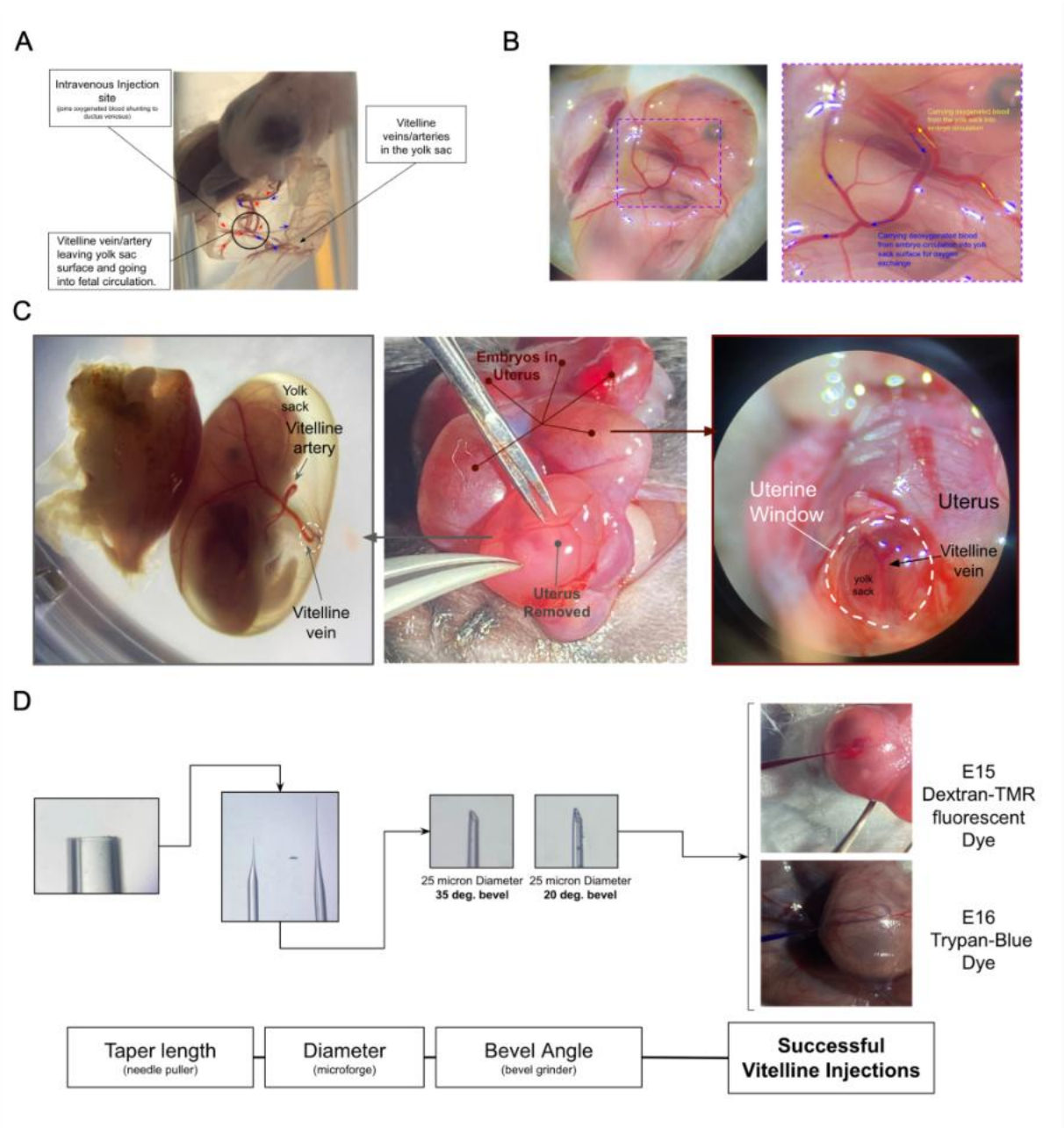

Figure 1. Surgical workflow, embryonic staging, and needle optimization for in utero vitelline injection.

(A) Ex utero *E15* mouse embryo following partial removal of the yolk sac. The injection site is indicated, and the vitelline vasculature is labeled, including vitelline arteries and veins extending from and coursing along the yolk sac surface. **(B)** *E15* embryo immediately after extraction from the uterus and still encased in the yolk sac (left). Major vessels are labeled according to

oxygenation status, with directional flow indicated by arrows. **(C)** Comparison of *E12–E12.5* surgical access. Left: embryo within intact yolk sac with vitelline artery and vein labeled. Middle: embryo partially protruding from the uterus during exposure of the uterine window. Right: microscope view of uterine window highlighting the yolk sac and vitelline vasculature at the injection site. **(D)** Schematic of injection needle optimization parameters, including taper length, outer diameter, and bevel angle, used to improve consistency and success of vitelline injections.

Figure 2: Systemic delivery to E15.5 and E12.5 embryo via uterine microdissection.

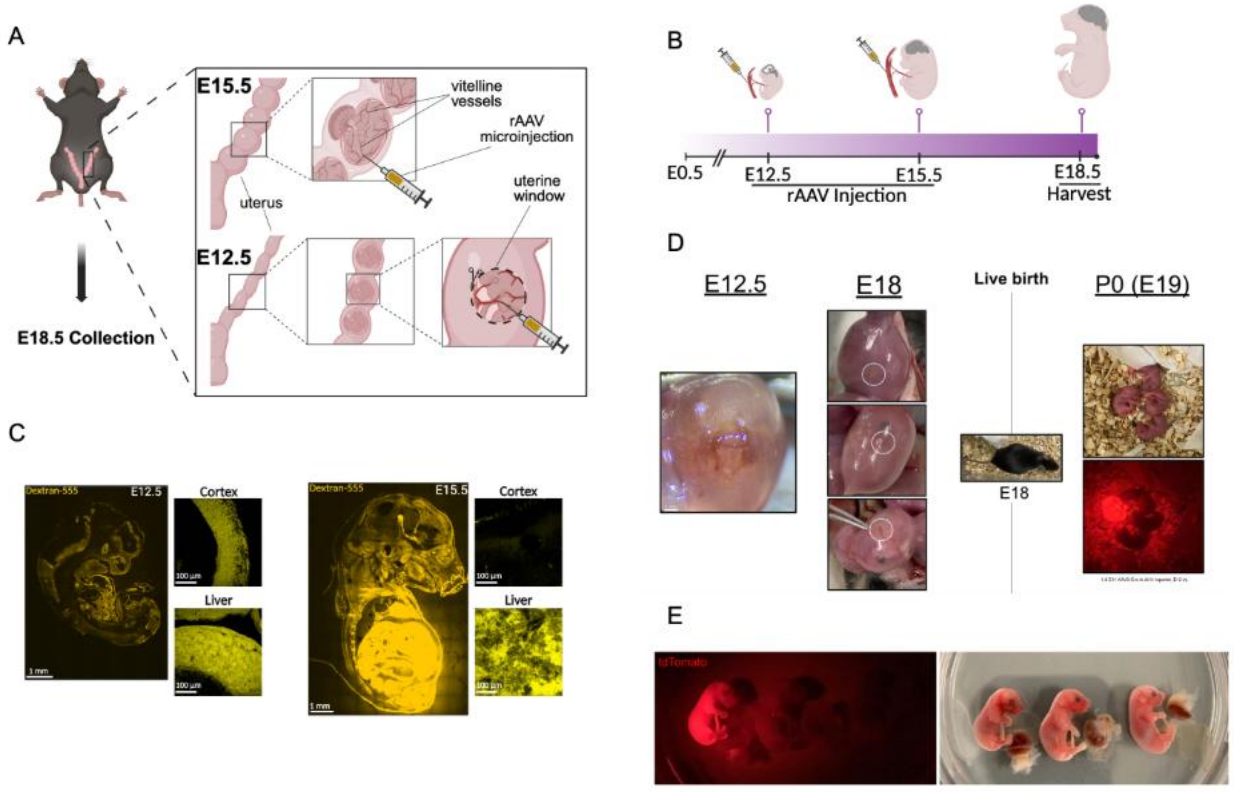

Figure 2. Systemic delivery to E15.5 and E12.5 embryos via uterine microdissection.

(A) Schematic of surgical techniques. E15.5 injection is performed through the uterus into the vitelline vein of the embryo. E12 injection requires microdissection of the opaque uterus to access the vitelline vein, followed by AAV microinjection. **(B)** Schematic illustrating the timeline of in utero AAV administration at E12.5 and E15.5, with embryo harvest at E18.5. **(C)** Fluorophore-conjugated dextran dye (555 nm, yellow) was injected through the vitelline vein. Embryos were collected within 1 hour of injection. Broad systemic distribution was observed in brain, heart, liver, lungs, and gut. Magnified images of E15.5 cortex and liver highlight dye uptake in organs of interest. Fluorescence intensity was normalized to liver intensity within each embryo (n = 2 embryos per stage). **(D)** E12.5 vitelline injection site accessed through uterine window, with representative healed uterine window scars observed at E18. Live birth survival at P0 and representative E12.5 AAV-Cre injected Ai14 embryo shown among uninjected littermates. **(E)** Representative E15 AAV-Cre injected Ai14 embryo shown among uninjected littermates.

3.5 Discussion

The results presented in Figures 1 and 2 establish a robust and reproducible framework for systemic intravascular delivery during early to midgestational stages of mouse development. A

key technical advance is the ability to access the vitelline circulation at E12.5 through uterine microdissection, effectively overcoming the longstanding limitation imposed by uterine opacity at early stages. As illustrated in Figure 1, precise anatomical identification of the vitelline vasculature, combined with optimized needle geometry, enables consistent vascular entry while minimizing tissue damage. Figure 2 demonstrates that this approach achieves rapid and widespread systemic distribution, as evidenced by dextran dye delivery across multiple organ systems, including the brain, liver, heart, and lungs. Notably, normalized fluorescence intensity signal highlights reproducible distribution patterns across embryos, supporting the reliability of this delivery method. The ability to achieve broad systemic exposure within one hour of injection underscores the efficiency of the vitelline route for rapid dissemination.

Importantly, successful delivery at E12.5 expands the accessible developmental window for genetic manipulation to a stage preceding extensive cortical differentiation. This enables targeting of progenitor populations during a critical phase of neurogenesis, which is not achievable with previously established E14+ approaches. Furthermore, the presence of live-born pups following uterine microdissection indicate that the procedure is compatible with continued embryonic development and littering of pups when performed carefully. The comparison between E12.5 and E15.5 injections also highlights stage-specific technical considerations. While E15.5 injections benefit from improved visualization and reduced need for tissue manipulation, E12.5 injections require greater surgical precision but offer access to earlier developmental processes. Together, these complementary approaches provide flexibility in targeting distinct developmental windows. In the context of genome editing, this platform offers significant advantages. Systemic AAV delivery via the vitelline vein enables widespread transduction, which is critical for applications requiring high coverage, such as CRISPR-based editing or recombinase activation. The demonstration of successful AAV-Cre activation in littered reporter embryos further validates the functional utility of this approach.

Overall, this work defines a permissive and previously inaccessible window for prenatal systemic delivery, bridging a critical technology gap between early embryonic development and later-stage fetal manipulation. By integrating surgical innovation with viral delivery strategies, this platform provides a powerful tool for studying developmental biology, modeling disease, and exploring early therapeutic interventions in vivo.

Chapter IV:

Prenatal CNS Capsid Engineering & Null Capsid Characterization

4.1 Summary

Efficient and targeted gene delivery to the developing brain remains a major barrier to advancing in utero gene therapy. Here, we characterize the biodistribution of systemic prenatal AAV delivery and identify developmental stage-dependent differences in capsid performance. We further evaluate natural and engineered serotypes across embryonic tissues and demonstrate that commonly used brain-biased capsids in adults fail to exhibit similar biases in the embryo. To address this limitation, we develop and validate "null" parent capsids with reduced native tropism and demonstrate that fusion with targeting motifs can partially restore receptor-mediated transduction. Finally, we apply a high-throughput barcoded capsid screening approach to perform iterative in vivo selections, identifying sequence features associated with improved brain enrichment. Together, these studies establish a framework for engineering AAV capsids with enhanced CNS specificity during early development.

4.2 Introduction

Recombinant adeno-associated viruses (rAAVs) are powerful tools for gene delivery due to their modularity and ability to transduce diverse cell types. While engineered capsids have enabled targeted delivery in adult tissues, achieving precise and efficient transduction in the developing embryo remains a challenge. In particular, systemic in utero vector delivery often results in widespread biodistribution, with strong off-target expression in organs such as the liver, limiting therapeutic specificity. Early embryonic stages present a unique opportunity for gene delivery, as developing tissues are more accessible and typically in a proliferative state. However, vector dilution, dynamic receptor expression, and developmental differences in tissue accessibility complicate efforts to achieve robust and selective brain targeting. As a result, there is a critical need to both characterize natural capsid behavior in the embryo and engineer new variants optimized for prenatal CNS delivery.

To address this, we first quantify biodistribution following systemic delivery at multiple developmental stages. We then compare natural and engineered serotypes in a pooled in vivo screen, revealing stage-specific differences in tropism. Building on these findings, we develop "null" capsids with reduced baseline transduction to serve as tunable backbones for targeted engineering. Finally, we perform iterative in vivo selection using a barcoded capsid library to identify variants with improved fetal brain enrichment (Figure 1).

4.3 Null-Parent Capsids for Decreased Off-target Transduction

A major limitation in AAV engineering is the inherently broad tropism of commonly used parent serotypes such as AAV9. This widespread transduction complicates efforts to achieve cell-type or organ-specific targeting, as engineering efforts rarely focus on reducing off-target expression rather than enhancing desired specificity. To overcome this, we explored the use of "null" capsids; variants identified from a 7-mer substitution library at the VR-I region that retain production efficiency but exhibit minimal transduction. These capsids are hypothesized to lack functional receptor interactions, effectively serving as detargeted scaffolds for further engineering.

We validated this concept by combining null mutations with the PHP.eB AA588 motif, which mediates entry via the Ly6a receptor. In vitro infectivity assays in Ly6a-expressing cells demonstrated that select Null–PHP.eB fusion capsids exhibit partially restored transduction, with increased infectivity in receptor-expressing cells compared to wild-type controls. These findings confirm that null capsids can serve as modular platforms, where receptor-specific targeting can be introduced without interference from native tropism (Figure 2).

In vivo validation further demonstrated that incorporation of the PHP.eB motif into null backgrounds enhances expression relative to null variants alone, supporting the feasibility of building targeted capsids from a detargeted starting point. This strategy enables more precise control over biodistribution and provides a foundation for engineering capsids with refined tissue specificity (Figure 3).

4.4 Lack of brain biased CNS vectors in the E12.5 and E15.5 Embryo

To determine whether existing AAV capsids exhibit brain specificity during development, we performed pooled in utero injections of seven natural and engineered serotypes at E15.5, followed by multi-organ NGS analysis. Despite prior reports of strong CNS tropism in adult animals, capsids such as PHP.eB, CAP-B10, and X1.1 did not show significant enrichment in embryonic brain tissues relative to AAV9. These findings highlight a fundamental disconnect between adult and embryonic tropism, likely driven by differences in receptor expression, tissue accessibility, and developmental biology. Importantly, systemic delivery at E15.5 resulted in broad biodistribution across organs, with no tested capsid demonstrating strong CNS bias. In contrast, earlier delivery at E12.5 resulted in increased brain enrichment, particularly for AAV9. Comparative analysis revealed a developmental stage-dependent shift in capsid distribution, with earlier injections favoring CNS accumulation. Histological analysis further supported these findings, showing that E12.5 delivery targets early progenitor populations and results in broader cortical coverage at later time points (Figure 4).

Together, these results demonstrate that both capsid identity and developmental timing are critical determinants of biodistribution, and that currently available capsids are insufficient for selective embryonic brain targeting.

4.5 AAV9 library selection for embryo CNS and organs of interest.

To identify capsids with improved embryonic brain tropism, we performed iterative in vivo selection using a barcoded AAV library targeting the AA588 variable region. Initial library characterization confirmed high sequence diversity and successful incorporation of variant motifs. In the first round of selection, variants were evaluated across multiple tissues and developmental stages (E12.5 and E15.5). Enrichment was defined based on consistent overrepresentation across biological replicates within a given majority condition. This approach enabled identification of variants with reproducible tissue-specific enrichment patterns.

Selected variants were used to generate a second-round library, to be re-injected and analyzed by NGS. Sequence similarity analysis revealed convergence among variants enriched in brain tissues, suggesting the emergence of shared structural or functional features driving CNS tropism. Comparative analysis across organs demonstrated that iterative selection reshapes capsid composition in a tissue-dependent manner, with distinct enrichment profiles observed in brain versus peripheral tissues. Notably, earlier developmental stages again favored brain enrichment, reinforcing the importance of injection timing (Figure 5).

This high-throughput screening strategy provides a scalable framework for identifying novel capsids with enhanced specificity and highlights the feasibility of engineering AAV variants optimized for prenatal CNS delivery.

4.6 Figures

Figure 1: Improved parent vector toward embryo CNS capsid engineering

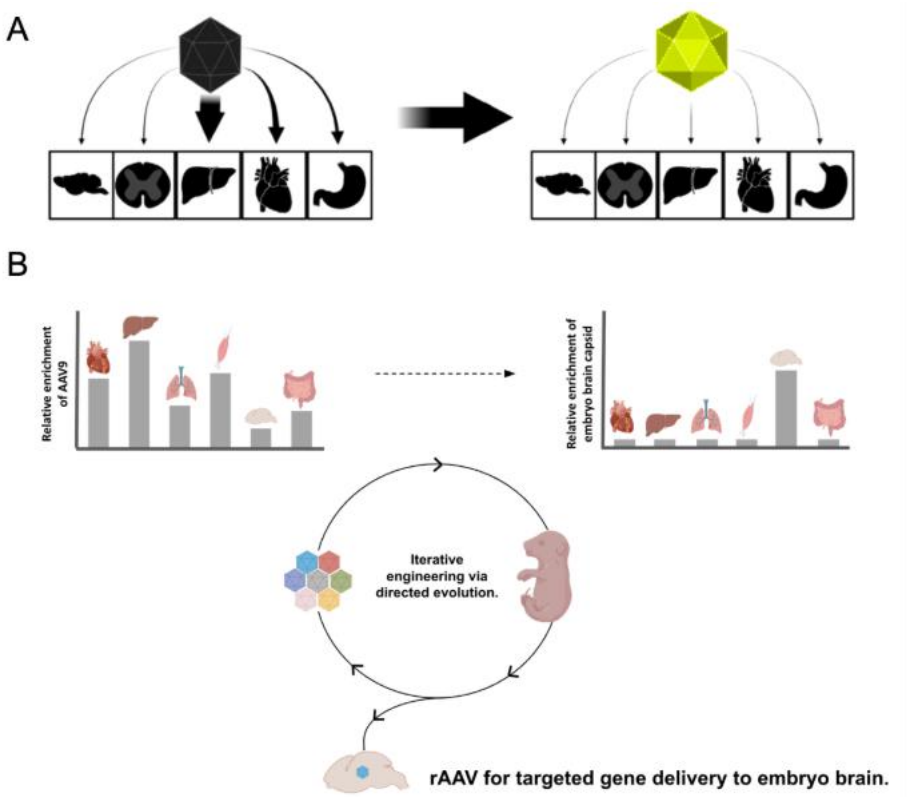

Figure 1. Improved parent vector toward embryo CNS capsid engineering. (A) Schematic illustrating the transition from the parental AAV9 capsid, which exhibits strong liver tropism, to a detargeted "null" capsid with reduced transduction across major peripheral organs. (B) Conceptual model of the desired organ enrichment profile, highlighting increased brain transduction alongside decreased off-target delivery to non-CNS tissues following capsid engineering. NGS data depicted are illustrative and not derived from experimental datasets. Lower panel schematic further outlines an iterative in utero engineering pipeline in the mouse embryo, enabling progressive selection of AAV variants with enhanced CNS penetrance at early developmental stages.

Figure 2: Null-PHP.eB fusion capsids exhibit partially restored tropism to Ly6a expressing cells

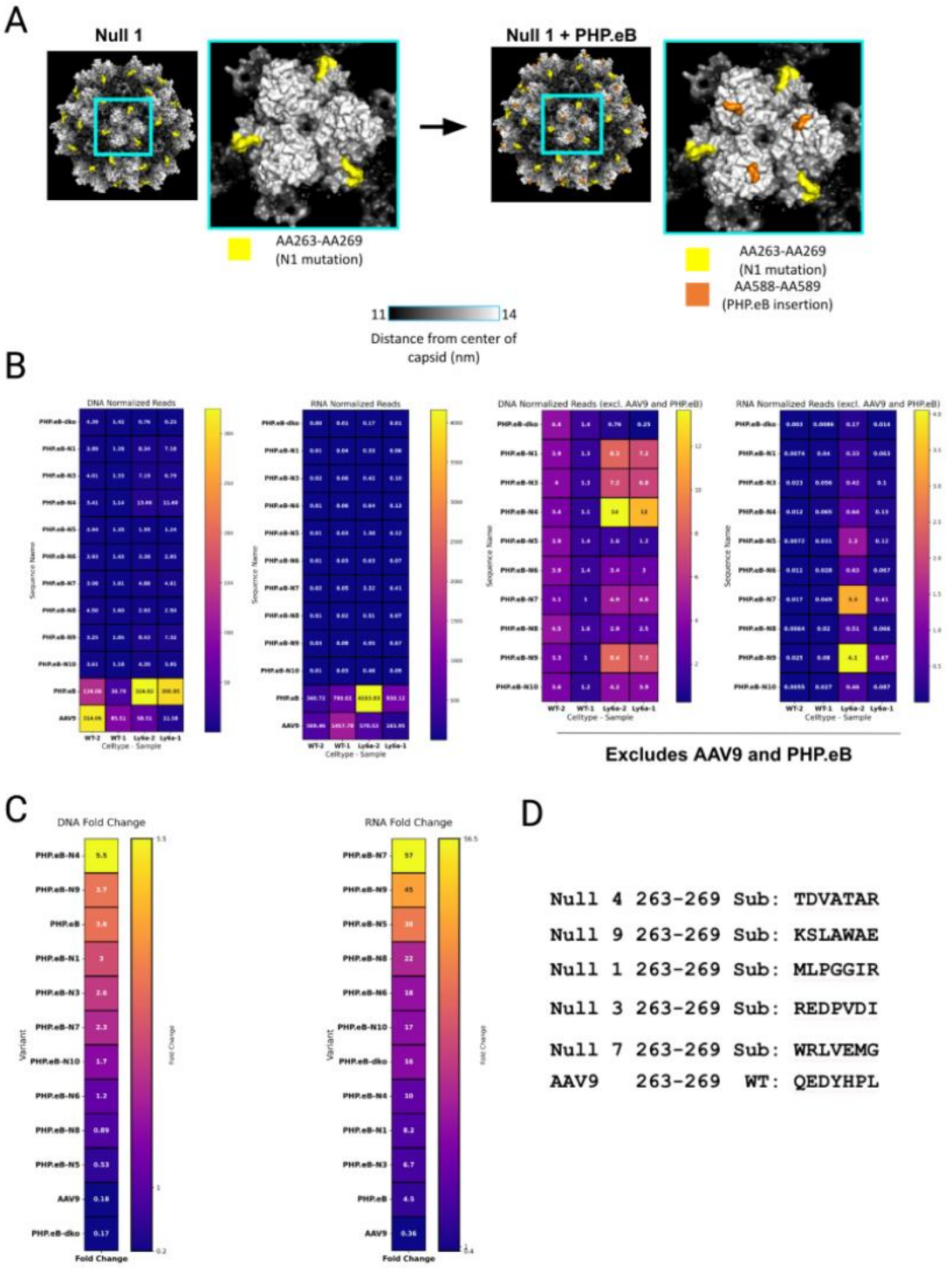

Figure 2. Null–PHP.eB fusion capsids exhibit partially restored tropism to Ly6a-expressing cells.

(A) Left, schematic of the null capsid highlighting the engineered mutation at amino acid position 262 (yellow). Right, design of the Null–PHP.eB fusion capsid incorporating the null 7-mer substitution at AA262 together with the PHP.eB insertion at AA588 (yellow). (B) Cell infectivity assay quantified by NGS, comparing null and fusion AAV capsids on cells expressing Ly6a, the receptor associated with PHP.eB-mediated entry. Experiments were performed in duplicate, and reads were normalized to the input library. (C) Ranked fold-change enrichment calculated from normalized reads in (B), defined as the differential transduction between wild-type cells and Ly6a-expressing cells for each capsid variant. (D) Sequences of the 7-mer substitutions at the AA262 position for each null capsid, shown relative to the AAV9 wild-type sequence.

Figure 3: Null-PHP.eB fusion capsid performance in vivo with direct injection.

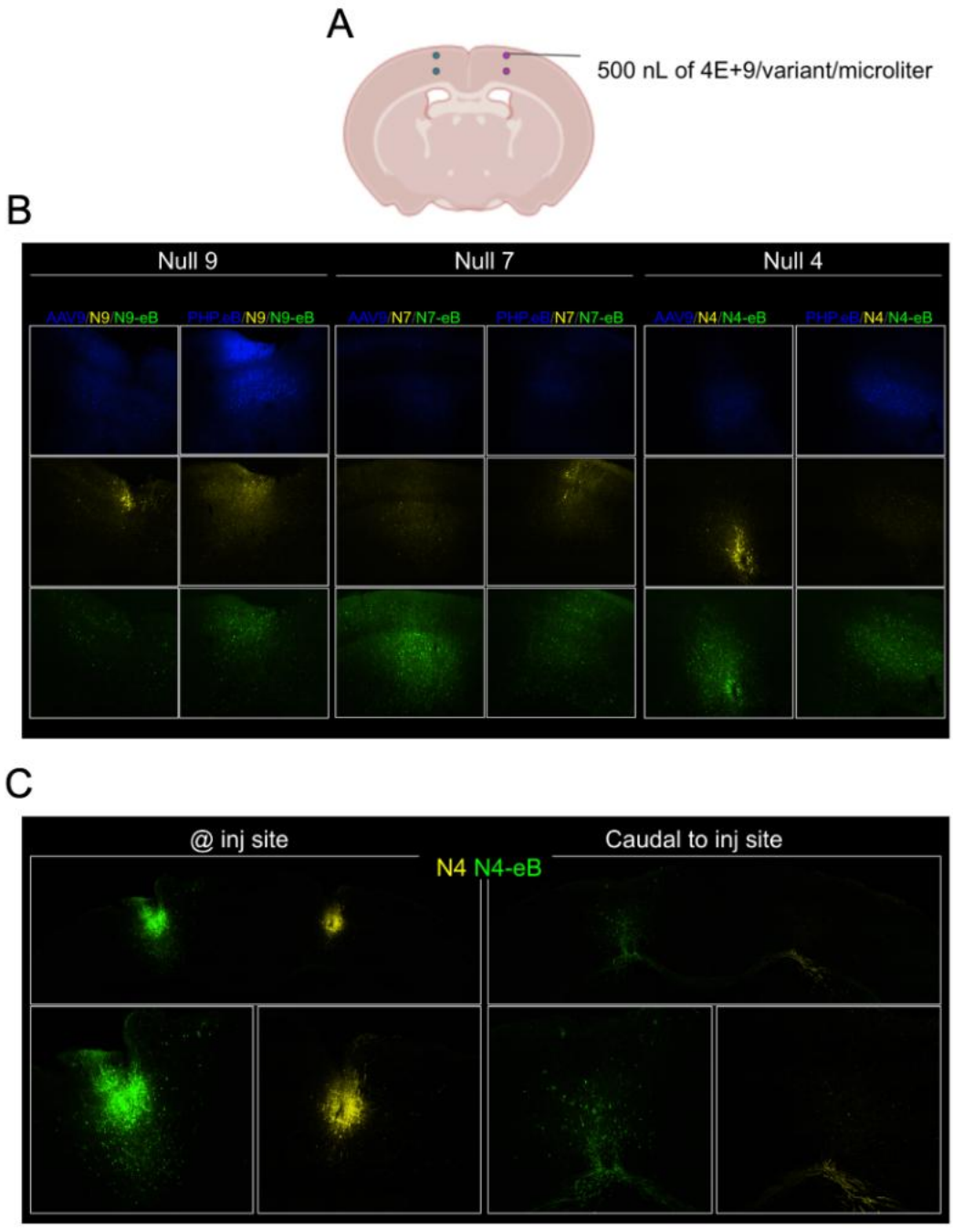

Figure 3. In vivo performance of Null–PHP.eB fusion capsids following direct cortical injection.

(A) Schematic of bilateral forebrain cortical injections, with distinct AAV variants delivered into each hemisphere for direct comparison. Two injection sites per hemisphere were used to enhance viral spread and minimize high local MOI at the injection site. (B) Co-injection strategy

consisting of pooled AAVs, including AAV9 or PHP.eB (blue), null variants (yellow), and null–PHP.eB fusion variants (green), enabling comparative assessment within the same tissue environment. (C) Comparison of N4 and N4-eB variants, demonstrating increased expression upon incorporation of the PHP.eB AA588 7-mer insertion into the null-4 backbone, relative to the N4 capsid retaining the wild-type sequence at AA588.

Figure 4: E12.5 and E15.5 natural and engineered serotype comparison across prenatal tissues.

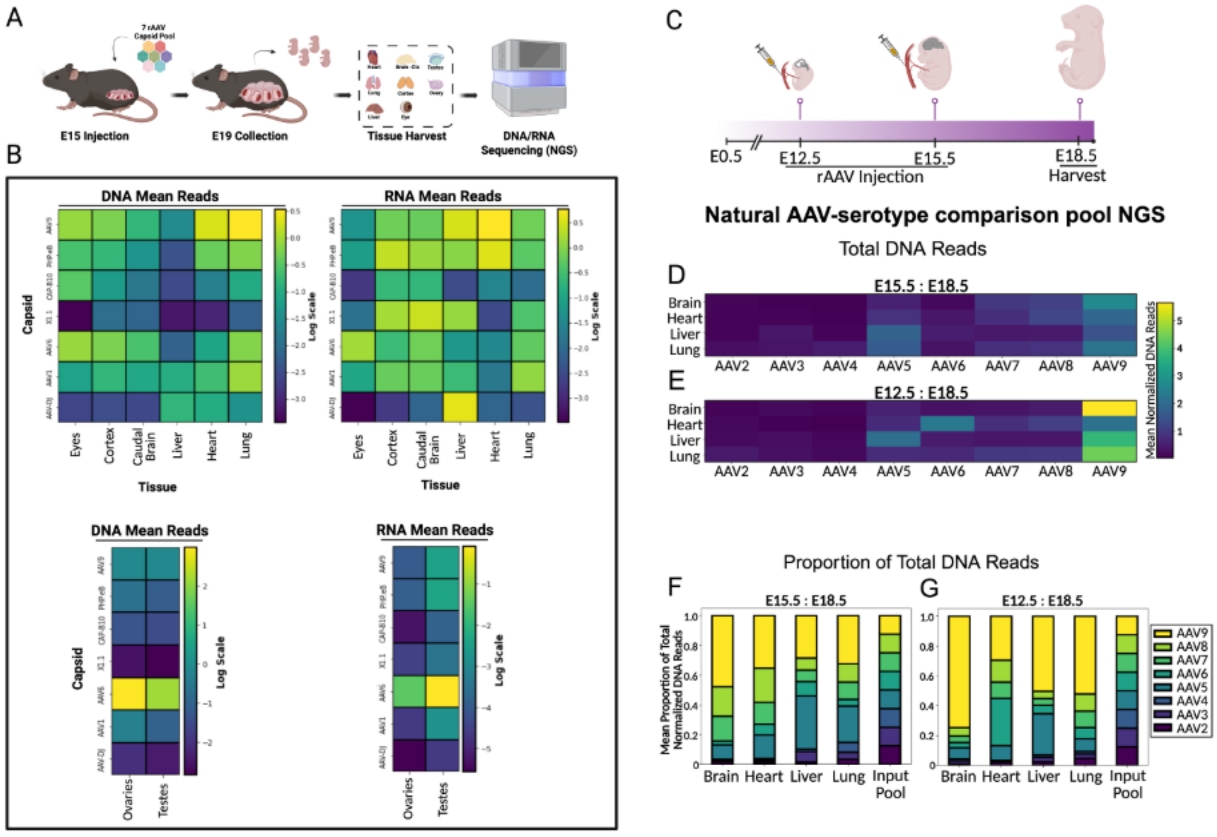

Figure 4. E12.5 and E15.5 natural and engineered serotype comparison across prenatal tissues.

(A) Schematic of the pooled in utero injection workflow, in which a barcoded capsid library is delivered to embryos, followed by late-gestation harvest, dissection of eight tissues, and NGS-based quantification. (B) Eight embryos were injected at E15.5 with an equimolar pool of seven barcoded capsids (AAV9, AAV-DJ, AAV1, AAV6, CAP-B10, PHP.eB, X1.1) and harvested at E18.5. Normalized DNA and RNA abundance for each capsid were quantified across cortex, caudal brain, eyes, liver, heart, and lung relative to AAV9. Data were analyzed using linear mixed-effects models with tissue, capsid, and normalized reads as fixed effects and biological replicate as a random effect (AAV9 as reference). Capsids previously reported to exhibit brain tropism in adult mice (PHP.eB, CAP-B10, X1.1) showed no statistically significant enrichment in CNS tissues nor depletion in liver (all $p > 0.05$). Normalized abundance in gonads (ovaries and testes; n = 2 female, n = 6 male) is also shown. (C) Schematic comparing E12.5 versus E15.5 in utero injection paradigms with a shared E18.5 harvest timepoint. (D-E) NGS analysis of the barcoded AAV library demonstrating developmental stage–dependent enrichment, with increased representation of AAV9 in the brain following earlier (E12.5) delivery (n = 3 embryos per stage). Vector genome counts were normalized to input library composition. (F-G) Stacked bar plots

showing the mean proportion of normalized reads per capsid at each developmental stage, derived from D–E, illustrating a shift in recovered capsid composition with increased AAV9 contribution to the brain after earlier embryonic injection.

Figure 5: 588-library selection in E15.5 and E12.5 embryos across tissues.

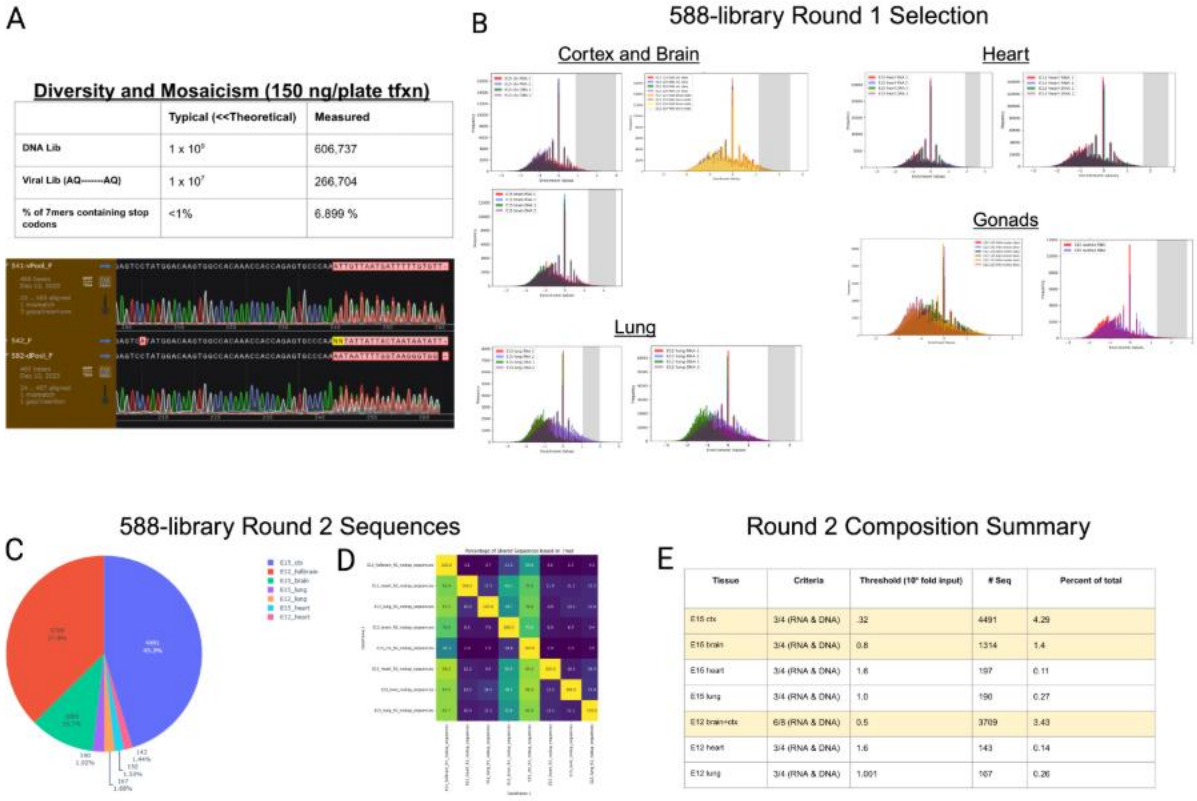

Figure 5. 588-library selection in E15.5 and E12.5 embryos across tissues. (A) Diversity metrics of the 588-library along with Sanger sequencing validation confirming successful insertion and sequence diversity in both the viral pool (vPool) and corresponding DNA pool (dPool). (B) Round 1 selection across organs and developmental stages (E15.5 and E12.5). Enrichment was defined by variants exceeding a threshold across the majority of tissue replicates within a condition (e.g., enrichment in ≥3/4 E12 cortex samples). (C) Composition of the Round 2 sequencing library following initial selection. (D) Sequence similarity analysis among variants enriched in brain and cortex tissues, highlighting convergence of selected motifs. (E) Summary of Round 2 capsid composition across each organ, illustrating tissue-specific enrichment patterns after iterative selection.

4.7 Discussion

This study highlights developmental stage as a critical and previously underappreciated determinant of AAV biodistribution in the embryo. As shown in **Figure 4**, systemic delivery at E15.5 results in broad, relatively non-specific transduction across multiple organs, with no engineered capsid demonstrating significant CNS enrichment despite prior validation in adult systems. In contrast, earlier delivery at E12.5 produces a marked shift in capsid distribution, with increased representation of AAV9 in the brain and reduced relative contribution from other serotypes. These findings suggest that temporal windows of accessibility, receptor expression, and tissue permeability strongly influence viral tropism, and that capsid performance must be evaluated within the developmental context in which it is intended to function.

The biodistribution data presented here also align with our histological observations described in Section 4.2, where E12.5 delivery leads to broader cortical coverage and targeting of early progenitor populations. Together, these results indicate that earlier intervention improves overall brain transduction and may enable access to cell populations that are otherwise difficult to target at later stages. However, even under these optimized conditions, no naturally occurring or engineered capsid tested exhibited strong brain specificity, reinforcing the need for de novo capsid engineering strategies for the fetal brain.

To address this limitation, we developed and validated null parent capsids as a foundation for refined targeting. As illustrated in Figure 1, the transition from a broadly tropic AAV9 capsid to a detargeted “null” variant represents a key conceptual shift in vector engineering. Rather than modifying a highly promiscuous capsid, null variants provide a minimal baseline with reduced off-target interactions. Functional validation of this approach is shown in Figure 2, where fusion of null capsids with the PHP.eB motif partially restores transduction in Ly6a-expressing cells. Importantly, these fusion variants exhibit increased specificity for receptor-expressing cells relative to wild-type backgrounds, supporting the hypothesis that null capsids can serve as modular scaffolds for receptor-driven targeting.

In vivo evaluation further supports this strategy. As shown in Figure 3, incorporation of the PHP.eB insertion into null variants enhances expression relative to null capsids alone following direct cortical injection. While these effects are modest and qualitative, they demonstrate that targeted functionality can be reintroduced onto a detargeted background, providing a pathway toward building capsids with improved specificity and reduced ectopic expression. This modular approach may be particularly valuable in the embryonic context, where broad systemic delivery amplifies the consequences of off-target transduction.

Building on these principles, we implemented an iterative in vivo selection strategy using a barcoded capsid library targeting the AA588 region. As shown in Figure 5, initial library characterization confirmed robust diversity, enabling effective sampling of sequence space.

Following Round 1 selection across tissues and developmental stages, enriched variants were used to generate a second-round library, resulting in convergence of sequence features among brain-enriched capsids. Notably, sequence similarity analysis revealed clustering of variants recovered from brain and cortex, suggesting that specific motifs may underlie CNS tropism in the embryo. Additionally, organ-level composition analyses demonstrate that selection pressures differ across tissues, enabling the identification of capsids with distinct enrichment profiles.

Importantly, the integration of developmental timing with high-throughput selection provides a powerful framework for capsid discovery. The stage-dependent differences observed in Figure 4, combined with the sequence convergence in Figure 5, suggest that optimal capsid features for brain targeting may be both temporally and biologically constrained. This highlights the importance of performing selection directly in the relevant physiological context, rather than relying solely on in vitro or adult models.

Overall, this work establishes a multi-layered strategy for engineering AAV vectors for prenatal CNS delivery. By combining (1) careful characterization of developmental biodistribution, (2) the use of null capsids to reduce baseline tropism, and (3) iterative in vivo selection to identify functional variants, we provide a roadmap for building next-generation vectors with improved specificity and efficacy. These advances have important implications not only for in utero gene therapy but also for basic neuroscience, where targeted access to defined cell populations in the developing brain remains a major challenge.

.

Chapter V:

Advancing Gene Editing in the Prenatal CNS, Genetic KO, epitope-tagging, and HDR insertion.

5.1 Summary

This chapter establishes a framework for efficient and precise in utero genome editing of the developing central nervous system during midgestation. By leveraging the favorable properties of AAV vectors and defining a cross-species developmental window aligned by cortical neurogenesis milestones, we identify a permissive stage for targeting neural progenitors with translational relevance to early human brain development. Systemic AAV delivery at midgestation enables widespread access to the embryonic cortex, as demonstrated by Cre-mediated lineage tracing and CRISPR-based genome editing. Using dual-sgRNA strategies, we show that efficient gene disruption can be achieved within days of delivery, producing robust editing outcomes prior to birth. Targeting of *Reln* recapitulates key features of cortical lamination defects, demonstrating that this approach can model neurodevelopmental disease phenotypes in vivo.

Beyond gene disruption, we demonstrate that homology-directed repair (HDR) can be harnessed in utero for precise genome editing, including endogenous protein tagging and installation of disease-associated human alleles. HDR-mediated modifications are observed across multiple cortical cell types, including both progenitors and differentiated neurons, indicating broad accessibility during this developmental window. Importantly, precise tagging of endogenous proteins is functionally tolerated, while pathogenic allele installation enables modeling of clinically relevant mutations in the embryonic brain. Together, these findings define midgestation as a critical window for prenatal genome engineering and establish a versatile platform for studying cortical development, modeling congenital disorders, and exploring early therapeutic interventions.

5.2 Introduction

Recombinant adeno-associated viruses (AAVs) are widely used for in utero gene therapy due to their low immunogenicity, safety profile, and ability to deliver diverse genetic payloads, including transgenes and genome editing tools. In the fetal context, AAV delivery is particularly advantageous: the immature immune system tolerates viral exposure well, and the small size of the fetus allows efficient systemic distribution at relatively low doses. However, achieving selective targeting remains challenging. Systemic delivery often leads to substantial off-target transduction, especially in the liver, limiting effective targeting of the developing central nervous system (CNS) and raising safety concerns.

Most prenatal AAV applications to date have relied on gene replacement, where therapeutic benefit depends on sustained transgene expression. In the developing fetus, this is complicated by rapid cell proliferation, which dilutes episomal AAV genomes and reduces expression over time. Genome editing offers a potential solution by enabling permanent genetic modification, particularly when targeting early progenitor populations. Although CRISPR-based in utero editing has been demonstrated, efficiencies in the brain remain low with systemic AAV delivery at midgestational stages, in part due to limited CNS access and preferential viral uptake by the liver. These findings suggest that developmental timing and vector choice are critical factors in successful prenatal gene delivery and editing.

Congenital disorders, particularly those affecting the CNS, represent a major unmet clinical need. The brain undergoes rapid and highly coordinated development during fetal stages, making it especially vulnerable to genetic disruptions. Malformations of cortical development are often driven by discrete genetic variants, yet prenatal diagnoses rarely translate into therapeutic intervention, and outcomes remain difficult to predict. This underscores the importance of developing strategies that enable both early functional studies and therapeutic manipulation within the developing brain.

Midgestation represents a promising but technically challenging window for intervention. During this period, neural progenitors expand and differentiate while the fetal liver matures, influencing viral distribution. Although early access to cortical progenitors is desirable, existing delivery approaches are limited by technical barriers, including difficulty visualizing embryonic vasculature prior to later stages. To overcome these constraints, we develop emerging strategies that combine refined surgical access with systemic AAV delivery to define a permissive window for efficient gene transfer and genome editing. These advances provide a foundation for studying cortical development, modeling neurodevelopmental disorders, and exploring early therapeutic interventions in utero.

5.3 Defining a Cross-Species Midgestational Window for In Utero Genome Editing

To establish a framework for studying and manipulating cortical development across species, we first defined mouse–human gestational equivalences based on cortex-specific developmental landmarks rather than overall embryonic age. Direct comparison between species is complicated by divergent developmental timing, but aligning key features such as neurogenesis onset, progenitor expansion, and laminar organization enables more meaningful cross-species translation. Using this approach, mouse embryonic day (E)12 corresponds approximately to human gestational weeks (GW) 7-10, a stage marked by early neurogenesis and the generation of deep-layer neurons. Mouse E15 aligns with GW10-14, characterized by peak deep-layer neurogenesis and expansion of cortical progenitor populations, while mouse postnatal day 0 (P0) approximates GW20-26, when cortical layers are largely established, and gliogenesis begins. These relationships define a midgestational window in the mouse that is developmentally analogous to early-mid human

cortical development and is therefore well suited for modeling disease-relevant processes (Figure 1A).

To further contextualize these interventions at the cellular level, we performed a meta-analysis of single-cell RNA sequencing (scRNA-seq) datasets spanning cortical development. Integration of publicly available datasets (Ruan et al., PNAS 2021; GSE161690; Fan et al., Sci Adv 2020; GSE120046; NCBI GEO) with additional compiled data (Meta-analysis, 2026) revealed distinct transcriptional programs associated with neural stem cell (NSC) maintenance and neuronal differentiation. NSC maintenance programs (purple) are defined by expression of canonical progenitor markers including SOX2, PAX6, and NES, whereas neuronal maturation programs (pan-neuronal; green) are characterized by expression of RBFOX3, MAP2, and SYN1 (Figure 1C). These signatures provide a molecular framework for assessing the impact of genome editing on lineage progression and cell state transitions in the developing cortex.

5.4 Midgestational Cre and dual sgRNA delivery enables prenatal CNS genome editing.

Cre recombinase is commonly used for conditional knockout of genes, either through viral delivery or Cre-driver transgenic lines. In the context of AAV delivery, Cre can also be used to assess viral tropism at different developmental stages using the Ai14 reporter line. Ai14 reporter mice, which carry a Cre-dependent tdTomato cassette; delivery of Cre during embryonic development activates tdTomato expression, marking infected progenitor cells and their progeny (Figure 2A).

Injection of AAV9-Cre into Ai14 mice at E12.5 and E15.5 led to widespread organ transduction, with the earlier delivery inducing more prominent RFP expression in the CNS (Figure 2B). The strong signal in the cortex and other brain regions demonstrates that midgestation viral delivery enables genome manipulation in the embryonic CNS prior to birth (Figure 2C, 2D). This supports the potential of this technique for efficient genome editing in the embryonic CNS prior to birth and suggests that midgestation viral delivery could be used to target neural progenitors for prenatal gene therapy.

To assess the efficacy of CRISPR-mediated genome editing following midgestational delivery, better understand the temporal dynamics of editing, and see how quickly the KO can occur; we evaluated a dual-sgRNA strategy designed to excise the Ai14 floxed stop cassette *in vivo*. Dual-sgRNA in a self-complimentary AAV9 vector was delivered *in utero* at E12.5 into Cas9/Ai14 embryos, and brains were harvested at E16.5 (96 hr post-injection) and E18.5 (144 hr post-injection) (Figure 2E).

Robust RFP expression was observed at both time points, consistent with efficient excision of the stop cassette. Quantification of RFP^+ cells, expressed as the percentage of $DAPI^+$ nuclei across multiple fetal brain regions, revealed substantial reporter activation in injected embryos compared to uninjected controls (n = 2 biologically independent embryos per condition) (Figure 2F). Editing was detectable as early as 96 hours post-injection. Representative cortical images demonstrated

widespread RFP-positive cells throughout the developing cortex following dual-sgRNA delivery (Figure 2G).

5.5 Midgestational AAV-CRISPR knockout of Reln disrupts cortical lamination in wildtype and Cas9-heterozygous mice

Conditional gene deletion using a Cre and floxed sequence relies upon the availability of a suitable mouse line. Programmable nucleases, such as Cas9, have a broad targeting capacity in wildtype animals, thereby increasing the space of sequences that can be assessed. Thus, we assessed whether midgestation delivery of CRISPR-Cas9 machinery to disrupt *Reln* would also yield a reeler-like cortical phenotype. To directly disrupt *Reln* during midgestation, sgRNAs targeting exon 1 of the locus were delivered via AAV9 into E12.5 embryos, which were allowed to develop *in utero* until E18.5. Dual sgRNA delivery into Cas9-expressing embryos, as well as co-injection of a dual sgRNA with SpCas9 into wildtype embryos, resulted in disrupted cortical lamination and a reeler-like phenotype (Figure 3). Both approaches caused a strong reduction in RELN+ cells within the marginal zone/layer I (MZ/LI) and across the imaged cortical region compared with uninjected controls, consistent with effective loss of functional Reelin protein. Both approaches also showed no reduction in BRN2+ cells compared to uninjected controls (Figure 3B). On average, dual sgRNA delivery and sgRNA/SpCas9 delivery caused a 40- and 9-fold reduction of RELN+ cells, respectively, compared to control cortices.

Layer-specific markers (Reelin for layer I, BRN2 for layers II/III, and CTIP2 for layer V) were used to evaluate laminar organization. In the absence of Reelin, deeper-layer CTIP2$^+$ neurons were displaced toward more superficial positions, while normally superficial BRN2+ neurons were less cohesive and shifted deeper. The Reelin-positive marginal zone was markedly reduced and nearly absent (Figure 3C-E). Spatial analysis using strip plots of individual neurons confirmed a reduced density of upper-layer BRN2+ neurons and mislocalization of deeper-layer CTIP2$^+$ neurons into superficial regions, highlighting profound laminar disruption following CRISPR-mediated *Reln* knockout (Figure 3F). These results demonstrate that midgestational AAV-CRISPR delivery can efficiently manipulate genes in the embryonic CNS, producing functional phenotypes before birth.

5.6 In utero HDR-mediated tagging and pathogenic allele installation demonstrate functional precision and broad cortical access

For therapeutic treatment and investigation of the developing embryo, many applications will require precision genome editting. We sought to assess the feasibility of homology-directed repair (HDR) for precise editing in multiple genes of interest. To evaluate access across cortical cell types, we targeted the endogenous *Actb* locus using a previously validated HDR donor and sgRNA [48] (derived from Addgene plasmid #119870) (Figure 4A). Midgestational delivery into Cas9 heterozygous embryos induced robust editing across the cortex. HA-positive cells included both SOX2-positive neural stem and progenitor cells and NeuN-positive mature neurons in cortex and

hippocampus (Figure 4B), indicating that AAV-delivered *in utero* HDR can access a wide range of cortical cell types spanning developmental states.

Building on our successful *Reln* cortical knockout, we used HDR to insert an HA epitope at the C-terminus of exon 63 of wild-type *Reln* (Figure 4C). This was achieved using a single guide RNA and HA-HDR donor packaged in AAV9. Cortical staining showed colocalization of HA and Reelin, indicating successful genome incorporation (Figure 4D). Tagging Reelin did not disrupt cortical lamination, as layers V and I were preserved relative to uninjected littermates, suggesting that Reelin-HA functions similarly to wild-type Reelin during cortical development. HA-positive cells were detected only in regions where Reelin is endogenously expressed, mainly the marginal zone (L-I) and hippocampus.

5.7 Modelling MCDs: HDR-mediated installation of clinically-relevant pathogenic allele in prenatal WT mouse cortex.

We next tested whether *in utero* HDR could install a human-derived pathogenic allele. We designed an AAV-HDR transgene encoding the patient-derived PDHA1 Tyr287fs frameshift mutation, which causes a mitochondrial disorder associated with malformations of cortical development (Figure 4E-F). Targeted sequencing confirmed insertion of the 4 bp. HDR frequency was higher in cortex than liver ($n = 3$, one-way ANOVA, $p = 0.0041$), and HDR reads were significantly enriched over WT and non-4 bp insertion classes in both tissues (one-way ANOVA with post-hoc correction, all $p < 0.05$, Figure 4G-H). Reads from uninjected littermates were almost exclusively of WT length ($n = 2$, Figure 4I-J).

Taken together, these data show that *in utero* AAV-HDR supports precise and functionally tolerated tagging of endogenous genes, and enables installation of pathogenic human-derived alleles in the developing cortex.

5.8 Figures

Figure 1: Developmental framework for midgestation in utero gene editing.

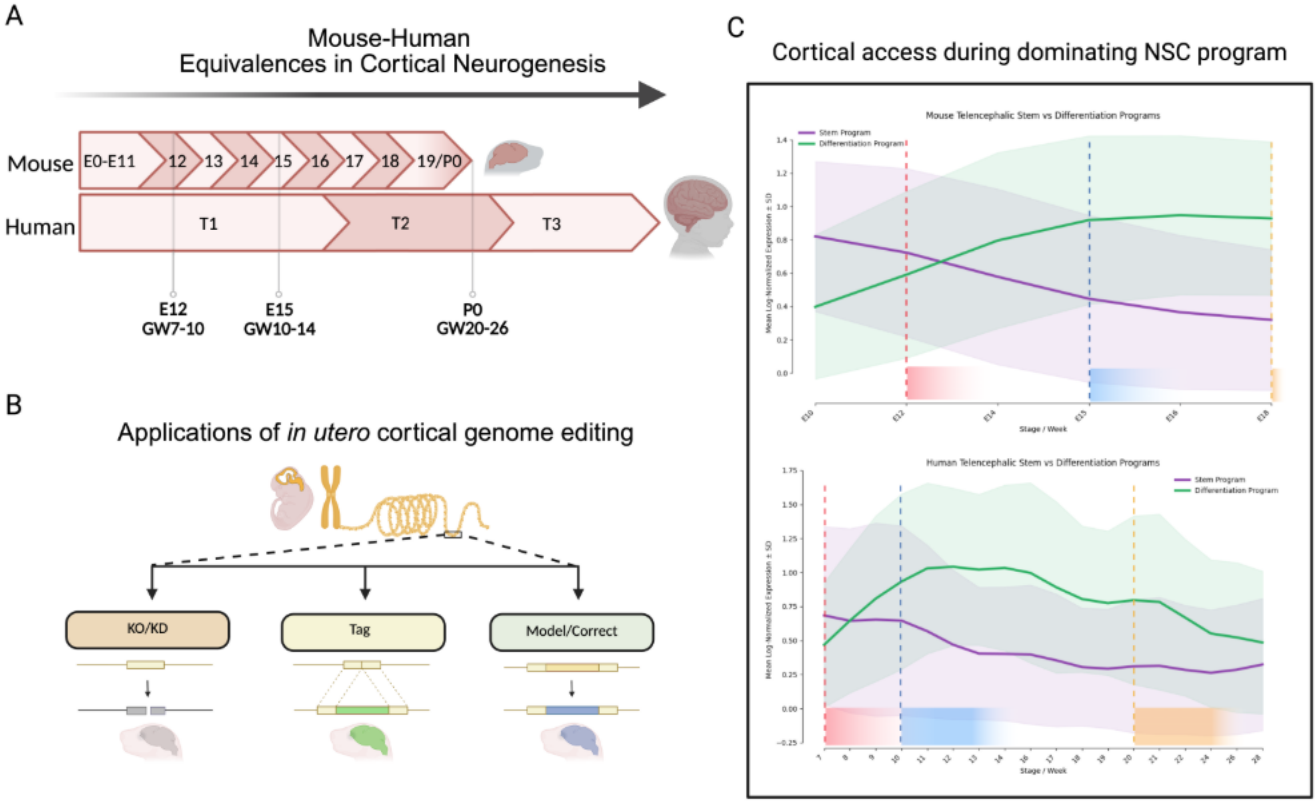

Figure 1: Developmental alignment and in utero genome editing strategies in the cortex.

(A) Mouse-human equivalences for cortical development derived from anatomical similarities and prenatal cell proliferation dynamics across species. (B) Applications of in utero genome editing in the developing cortex, with schematic representations of gene knockout (KO), epitope tagging, and targeted gene correction. (C) Single-cell RNA sequencing (scRNA-seq) meta-analysis of cortical neural stem cell (NSC) maintenance versus neuronal differentiation programs, integrating datasets from Ruan et al. (PNAS 2021; GSE161690), Fan et al. (Sci Adv 2020; GSE120046), and additional publicly available datasets (NCBI GEO; Meta-analysis, 2026). NSC maintenance programs (purple) are characterized by expression of SOX2, PAX6, and NES, while neuronal maturation programs (pan-neuronal; green) are marked by RBFOX3, MAP2, and SYN1.

Figure 2: Systemic AAV9-Cre delivery enables prenatal genome recombination in the embryonic brain.

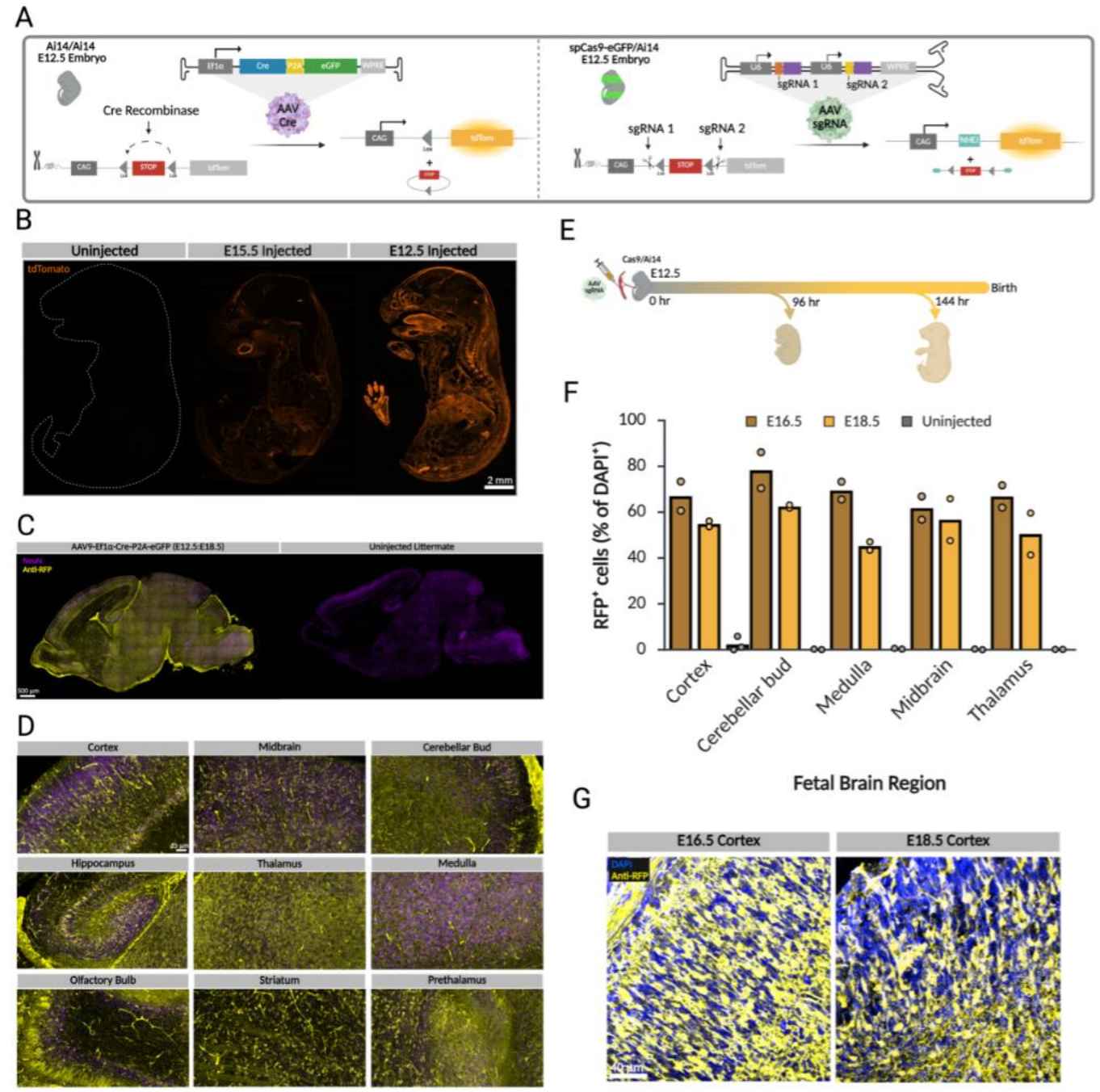

Figure 2: Systemic AAV9-Cre delivery enables prenatal genome recombination in the embryonic brain.

A) Schematic of the Ai14 reporter allele. A loxP-flanked transcriptional stop cassette prevents tdTomato expression from the CAG promoter. In the left panel, delivery of AAV9-Cre excises the stop cassette, enabling tdTomato expression. In the right panel, dual sgRNAs targeting sequences flanking the stop cassette are delivered into Cas9/Ai14 mice, resulting in CRISPR-Cas9-mediated excision of the stop cassette and subsequent tdTomato expression. **B)** Sagittal sections of E18.5 embryos injected with AAV9-Cre at E12.5 or E15.5, showing widespread tdTomato expression across multiple organs. Expression is generally stronger following E12.5 delivery, with noticeable labeling in the brain (n = 3 embryos per stage). **C)** Sagittal sections of P0 brains from injected and uninjected embryos, stained with NeuN and anti-RFP antibodies, showing tdTomato expression in neurons after *in utero* AAV9-Cre delivery (n = 2 embryos per stage). **D)** 25x images of various labeled brain regions from C, illustrating that AAV9-Cre transduced the progenitors of cortical and non-cortical brain areas. **E)** Schematic of in utero injection of dual-sgRNA scAAV9 at embryonic day 12.5 (E12.5; 0 hr). Embryos were harvested at E16.5 (96 hr post-injection) and E18.5 (144 hr post-injection) to assess CRISPR-mediated excision efficiency. **F)** Quantification of RFP^+ cells, expressed as the percentage of $DAPI^+$ nuclei, across multiple fetal brain regions in uninjected controls and embryos harvested at E16.5 and E18.5 following dual-sgRNA delivery. n = 2 biologically independent embryos per condition. **G)** Representative cortical images showing RFP-expressing cells at E16.5 and E18.5 (40×) following dual-sgRNA injection.

Figure 3: AAV-CRISPR-mediated knockout of *Reln* in midgestation disrupts cortical lamination in wildtype and Cas9-heterozygous mice.

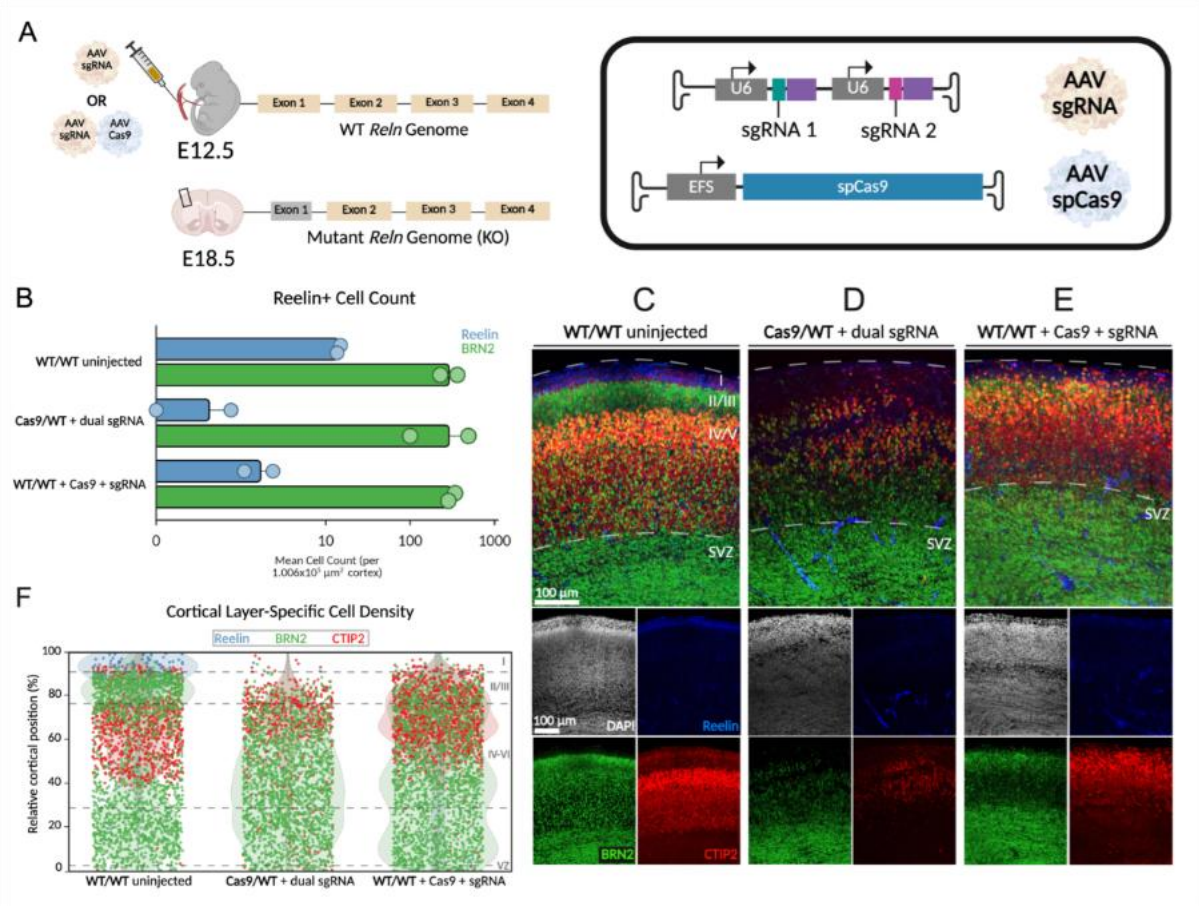

Figure 3: AAV-CRISPR-mediated knockout of *Reln* in midgestation disrupts cortical lamination in wildtype and Cas9-heterozygous mice.

A) Schematic of AAV-CRISPR microinjection at E12.5. Dual-guide AAV vectors (sgRNA) were delivered into heterozygous Cas9/wildtype (WT) embryos, or co-delivered with an AAV-Cas9 vector (spCas9 under the EFS promoter) in WT embryos. All transgenes were packaged in an AAV9 capsid. **B)** Quantification of Reelin- and Brn2-positive cortical cells at E18.5 following AAV delivery at E12.5 (n = 2 animals per condition). Values are shown on a log scale. Injected conditions exhibit a reduction in Reelin+ cells compared to uninjected wildtype controls. **C-E)** Representative cortical images spanning the subventricular zone (SVZ) to marginal zone (MZ). Layer-specific markers were used for lamination assessment: Reelin (LI, blue), BRN2 (LII/III and SVZ, green), and CTIP2 (LIV/V, red). **F)** Relative positions of Reelin-, BRN2-, and CTIP2-positive cells plotted as a percentage of total cortical height, illustrating altered cortical organization and reduced Reelin+ cell populations in injected embryos compared to uninjected controls.

Figure 4: *In utero* HDR-mediated tagging and pathogenic allele installation.

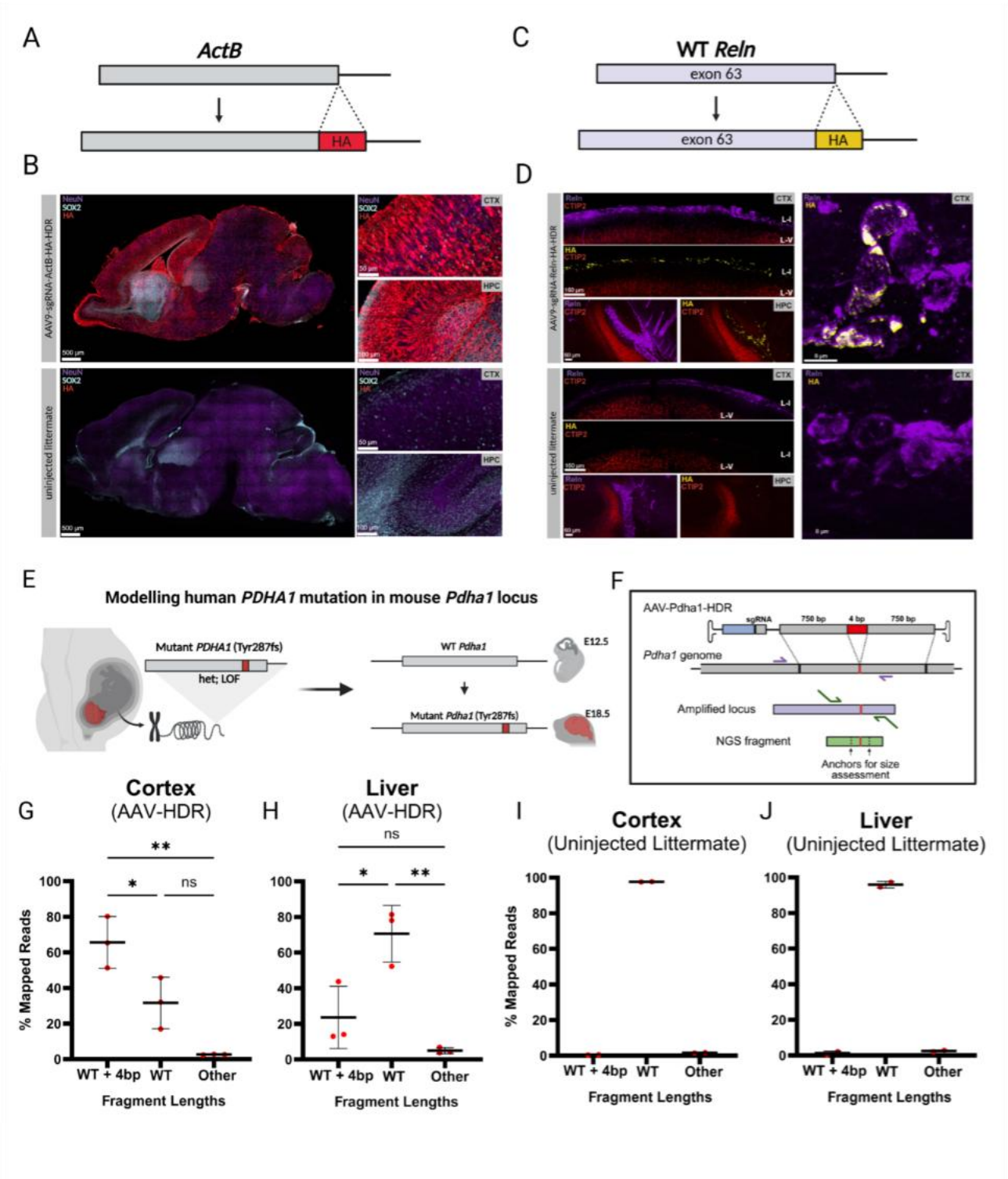

Figure 4: *In utero* HDR-mediated tagging and pathogenic allele installation.

A) Schematic of HDR-mediated insertion of an HA tag at the C-terminus of WT β-actin (*Actb*). **B)** Immunostaining of NeuN (purple), HA (red), and Sox2 (teal) in sagittal brain sections from

Actb-tagged embryos and uninjected littermates, with higher magnification images of cortex (CTX) and hippocampus (HPC) below. **C)** Schematic of HDR-mediated insertion of an HA tag at the C-terminus of wild-type (WT) *Reln* exon 63, with 750-bp homology arms. **D)** Immunostaining for HA (yellow), Reelin (purple), and CTIP2 (red) in E18.5 cortex from Cas9/WT heterozygous embryos. E12.5-injected embryos show HA expression confined to cortical regions (CTX) where Reelin is expressed, predominantly in the marginal zone (L-I) and hippocampus (HPC). Minimal HA signal was detected in uninjected littermate controls. **E)** Schematic of HDR-mediated incorporation of a human patient-derived PDHA1 Tyr287fs mutation into Cas9/WT heterozygous mouse embryos (WT at the *Pdha1* locus). **F)** AAV transgene HDR design and Pdha1 locus amplification diagram. Sequenced NGS fragments analized for HDR incorporation using distance between two anchor sequences within the fragment (64 bp distance between anchors in WT genome). **G-H)** Distribution of reads classified as WT+4bp (HDR 4-bp insertion), WT (no insertion), or "Other" (non-4-bp edits) in injected cortex and liver, plotted as percentage of total reads. HDR insertions significantly exceed WT and other classes (all $p < 0.05$) in both tissues. ($n = 3$ embryos). Cortex displays significantly higher insertion frequency than liver ($p = 0.0041$). **I-J)** Equivalent analysis performed for uninjected cortex and liver ($n = 2$), showing minimal HDR-like insertion events.

5.9 Discussion

Efficient prenatal genome manipulation using Cre and CRISPR-based approaches

Leveraging this permissive window, we demonstrated efficient genome manipulation in the embryonic CNS using both Cre-lox and CRISPR-based strategies. Systemic AAV9-mediated delivery of Cre recombinase to Ai14 reporter embryos resulted in widespread recombination across multiple organs by E18.5, with particularly high penetrance in the brain following E12.5 administration. Because recombination affects both infected progenitors and their progeny, this approach provides a rapid and scalable alternative to Cre driver lines for CNS-specific genome manipulation prior to birth [53].

Importantly, the dual-sgRNA strategy enables deletion of exon-sized genomic fragments through Cas9-mediated excision between two guide RNA target sites. This approach extends prenatal genome manipulation beyond Cre-lox recombination by permitting precise programmable gene disruption in the embryonic CNS. The ability to induce defined deletions in neural progenitors during midgestation supports the feasibility of in utero CRISPR-based gene knockout strategies and provides a framework for modeling neurodevelopmental disorders or exploring prenatal therapeutic genome editing.

Beyond reporter systems, we demonstrated functional genome disruption by targeting *Reln*, a gene essential for cortical lamination [54]. Both conditional deletion of *Reln* via AAV9-Cre delivery as well as AAV-CRISPR-mediated knockout initiated at E12.5 were sufficient to induce a prenatal reeler-like phenotype. Edited embryos exhibited loss of Reelin-positive marginal zone cells, redistribution of deep-layer neurons, and disrupted cortical lamination consistent with classical reeler pathology [55]. These findings establish that midgestational genome manipulation can perturb core neurodevelopmental programs prior to birth in otherwise wild-type animals.

A practical advantage of this platform is the use of Cas9-expressing stud males crossed with wild-type females, producing embryos with heterozygous Cas9 expression. As the pregnant females were terminal, this strategy is both cost-effective and scalable, facilitating efficient generation of somatically edited embryos without the requirement for maintaining complex transgenic breeding colonies. While germline editing is possible, it was not systematically assessed in this study and remains an important area for future evaluation.

Precision genome modification via HDR in the embryonic CNS

In addition to gene disruption, we demonstrated the feasibility of precise genome modification via HDR *in vivo*. HA tagging of endogenous *Reln* preserved protein localization and cortical lamination, indicating that C-terminal tagging did not compromise Reelin function during corticogenesis. Extension of this strategy to the *Actb* locus revealed robust and widespread cortical

access, with successful HA knock-in observed in neural progenitors and differentiated neurons across the cortex and hippocampus. Precise editing by HDR is particularly well suited to this developmental context, as the E12.5 cortex is dominated by rapidly dividing neural progenitors that have more capacity for HDR [56, 57]. Together, these results establish HDR-based editing as a viable strategy for endogenous gene tagging and disease modeling in the embryonic CNS.

Modeling prenatal cortical disorders and clinical relevance

The ability to manipulate the embryonic genome systemically and assess phenotypes prior to birth has direct relevance for modeling congenital neurodevelopmental disorders. Many pathogenic variants identified through prenatal screening, particularly those associated with malformed cortical development, exhibit variable penetrance and uncertain postnatal manifestation [58]. The majority of prenatally diagnosed cortical malformations are associated with single nucleotide or copy number variants [10], underscoring the need for precise functional modeling. Guided by these observations, we modeled a human pathogenic four-base-pair insertion in the PDHA1 locus associated with prenatal malformation of cortical development, using HDR-mediated editing. This approach enables recapitulation of disease-associated alleles *in vivo* and allows direct assessment of developmental consequences during corticogenesis. *In utero* modeling could provide a powerful framework for phenocopying early human neurodevelopment prior to term, offering insight into how specific genetic lesions may translate into postnatal disability.

Gestational equivalence and translational interpretation

Direct comparison between mouse and human gestational timelines remains challenging due to species-specific differences in brain development. Rather than relying on global embryonic age, we define gestational equivalences using cortex-specific developmental and neurogenesis milestones. Using this framework, mouse E12 corresponds approximately to human gestational weeks (GW) 7-10, characterized by early neurogenesis and the birth of deep-layer neurons [59, 60]. Mouse E15 aligns with GW10-14, a period of peak deep-layer neurogenesis and expanding progenitor populations, while mouse P0 approximates GW20-26, when cortical layers are established and gliogenesis begins [61, 62]. Thus, the midgestational mouse interventions we describe here offer translational relevance for modeling early human cortical development.

Technical challenges and sources of experimental variability

Despite the advances we describe here, *in utero* gene delivery remains technically challenging. We observed embryonic lethality associated with excessive uterine manipulation, prolonged exposure leading to tissue desiccation, uterine contortion, or obstruction of placental blood flow. Creation of an injection site that was too large resulted in embryonic inviability, likely due to loss of amniotic integrity or hemorrhage. Maternal morbidity also posed a significant limitation. Dams that failed to carry embryos to term often exhibited near-necrotic intestines and marked fecal

accumulation at necropsy, suggestive of ileus or intestinal damage incurred during surgery. These findings emphasize the importance of minimizing operative duration and tissue disruption.

A further source of variability in our experiments arose from embryonic staging. Although injections were performed at midday on E12 based on plug detection, we observed apparent developmental stages ranging from E11.5 to E13.5, likely reflecting variation in copulation timing during the nocturnal active phase and differences in embryo number. Given the stage-dependent nature of cortical development and genome editing efficiency, more precise methods of tracking gestational time would aid future experiments.

Bibliography

1. [R1] Deverman, B. E., Pravdo, P. L., Simpson, B. P., Kumar, S. R., Chan, K. Y., Banerjee, A., Wu, W. L., Yang, B., Huber, N., Pasca, S. P., Gradinaru, V. (2016). Cre-dependent selection yields AAV variants for widespread gene transfer to the adult brain. *Nature Biotechnology, 34*(2), 204–209. https://doi.org/10.1038/nbt.3440
2. [R2] Asokan, A., Schaffer, D. V., & Samulski, R. J. (2012). The AAV vector toolkit: poised at the clinical crossroads. *Molecular Therapy, 20*(4), 699–708. https://doi.org/10.1038/mt.2011.287
3. [R3] Wang, D., Tai, P. W. L., & Gao, G. (2019). Adeno-associated virus vector as a platform for gene therapy delivery. Nature Reviews Drug Discovery, 18(5), 358–378. https://doi.org/10.1038/s41573-019-0012-9
4. [R4] Weinmann, J., Weis, S., Sippel, J., Tulalamba, W., Remes, A., El Andari, J., Herrmann, A. K., Pham, Q. H., Borowski, C., Hille, S., Jurado-Arjona, J., Kummer, M. P., & Grimm, D. (2020). Identification of a myotropic AAV by massively parallel in vivo evaluation of barcoded capsid variants. *Nature Communications, 11*, 5432. https://doi.org/10.1038/s41467-020-19230-w
5. [R5] Fischer KB, Collins HK, Callaway EM. Sources of off-target expression from recombinase-dependent AAV vectors and mitigation with cross-over insensitive ATG-out vectors. Proc Natl Acad Sci U S A. 2019 Dec 26;116(52):27001-27010. doi: 10.1073/pnas.1915974116. Epub 2019 Dec 16. PMID: 31843925; PMCID: PMC6936690.
6. [R6] Wang, J.-H., Zhan, W., Gallagher, T. L., & Gao, G. (2024). Recombinant adeno-associated virus as a delivery platform for ocular gene therapy: A comprehensive review. *Molecular Therapy*, 32(12), 4185–4207. https://doi.org/10.1016/j.ymthe.2024.10.017
7. [1] DeSilva, M., et al. (2016). Congenital anomalies: Case definition and guidelines for data collection, analysis and presentation for congenital anomalies as adverse events following immunization. *Journal of Epidemiology and Global Health, 6*(1), 65–76. https://doi.org/10.1016/j.jegh.2015.12.001
8. [2] Silbereis, J. C., Pochareddy, S., Zhu, Y., Li, M., & Sestan, N. (2016). The cellular and molecular landscapes of the developing human central nervous system. *Neuron, 89*(2), 248–268. https://doi.org/10.1016/j.neuron.2015.12.008
9. [3] Konrad, K., Firk, C., & Uhlhaas, P. J. (2013). Brain development during adolescence. *Frontiers in Human Neuroscience, 7*, 1–12. https://doi.org/10.3389/fnhum.2013.00850
10. [4] Leibovitz, Z., Lerman-Sagie, T., & Haddad, L. (2022). Fetal brain development: Regulating processes and related malformations. *Life, 12*(6), 809. https://doi.org/10.3390/life12060809
11. [5] Wu, Y., De Asis-Cruz, J., & Limperopoulos, C. (2024). Brain structural and functional outcomes in the offspring of women experiencing psychological distress during pregnancy. *Molecular Psychiatry, 29*, 2223–2240. https://doi.org/10.1038/s41380-024-02449-0

12. [6] Miguel, P. M., Pereira, L. O., Silveira, P. P., & Meaney, M. J. (2019). Early environmental influences on the development of children's brain structure and function. *Developmental Medicine & Child Neurology, 61*(10), 1127–1133. https://doi.org/10.1111/dmcn.14182
13. [7] Aydın, E., Tanacan, A., Büyükeren, M., Uçkan, H., Yurdakök, M., & Beksaç, M. S. (2019). Congenital central nervous system anomalies: Ten-year single center experience on a challenging issue in perinatal medicine. *Journal of the Turkish-German Gynecological Association, 20*(3), 170–177. https://doi.org/10.4274/jtgga.galenos.2018.2018.0079
14. [8] Wang, Y., Sun, X., & Xu, Z. (2022). Fetal Brain Development: Regulating Processes and Related Malformations. *Frontiers in Cellular Neuroscience*, 16, 924340. doi: 10.3390/life12060809
15. [9] Parrini, E., Conti, V., Dobyns, W. B., & Guerrini, R. (2016). Genetic basis of brain malformations. *Molecular Syndromology, 7*(4), 220–233. https://doi.org/10.1159/000448639
16. [10] Wang, L. L., Pan, P. S., Ma, H., He, C., Qin, Z. L., He, W., Huang, J., Tan, S. Y., Meng, D. H., Wei, H. W., & Yin, A. H. (2024). Malformations of cortical development: Fetal imaging and genetics. *Molecular Genetics & Genomic Medicine, 12*(4), e2440. https://doi.org/10.1002/mgg3.2440
17. [11] Peranteau, W. H., & Flake, A. W. (2020). The future of in utero gene therapy. *Molecular Diagnosis & Therapy, 24*(2), 135–142. https://doi.org/10.1007/s40291-020-00445-y
18. [12] O'Connell, A. E., Guseh, S., Lapteva, L., et al. (2020). Gene and stem cell therapies for fetal care: A review. *JAMA Pediatrics, 174*(10), 985–991. https://doi.org/10.1001/jamapediatrics.2020.1519
19. [13] Cohen, J. L., Chakraborty, P., et al. (2022). In utero enzyme-replacement therapy for infantile-onset Pompe's disease. *New England Journal of Medicine.* https://doi.org/10.1056/NEJMoa2200587
20. [14] Garrett, D. J., Larson, J. E., Dunn, D., Marrero, L., & Cohen, J. C. (2003). In utero recombinant adeno-associated virus gene transfer in mice, rats, and primates. *BMC Biotechnology, 3*, 16. https://doi.org/10.1186/1472-6750-3-16
21. [15] Mattar, C. N. Z., Gil-Farina, I., Rosales, C., Johana, N., Tan, Y. Y. W., McIntosh, J., Kaeppel, C., Waddington, S. N., Biswas, A., Choolani, M., Schmidt, M., Nathwani, A. C., & Chan, J. K. Y. (2017). In utero transfer of adeno-associated viral vectors produces long-term Factor IX levels in a cynomolgus macaque model. *Molecular Therapy, 25*(8), 1843–1853. https://doi.org/10.1016/j.ymthe.2017.04.003
22. [16] Challis, R. C., Kumar, S. R., Chen, X., Goertsen, D., Coughlin, G. M., Hori, A. M., Chuapoco, M. R., Otis, T. S., Miles, T. F., & Gradinaru, V. (2022). Adeno-associated virus toolkit to target diverse brain cells. *Annual Review of Neuroscience, 45*, 447–469. https://doi.org/10.1146/annurev-neuro-111020-100834

23. [17] Coughlin, G. M., Borsos, M., Barcelona, B. H., et al. (2025). Spatial genomics of AAV vectors reveals mechanism of transcriptional crosstalk that enables targeted delivery of large genetic cargo. *Nature Biotechnology, 44*, 133–145. https://doi.org/10.1038/s41587-025-02565-4
24. [18] Riley, J. S., Luks, V. L., Berkowitz, C. L., et al. (2024). Preexisting maternal immunity to AAV but not Cas9 impairs in utero gene editing in mice. *Journal of Clinical Investigation, 134*(12), e179848. https://doi.org/10.1172/JCI179848
25. [19] Hudry, E., & Vandenberghe, L. H. (2019). Therapeutic AAV gene transfer to the nervous system: A clinical reality. *Neuron, 101*(5), 839–862. https://doi.org/10.1016/j.neuron.2019.02.017
26. [20] Waddington, S. N., Peranteau, W. H., Rahim, A. A., Boyle, A. K., Kurian, M. A., Gissen, P., Chan, J. K. Y., & David, A. L. (2024). Fetal gene therapy. *Journal of Inherited Metabolic Disease, 47*(1), 192–210. https://doi.org/10.1002/jimd.12659
27. [21] Wang, D., Tai, P. W. L., & Gao, G. (2019). Adeno-associated virus vector as a platform for gene therapy delivery. *Nature Reviews Drug Discovery, 18*(5), 358–378. https://doi.org/10.1038/s41573-019-0012-9
28. [22] High, K. A., & Roncarolo, M. G. (2019). Gene therapy. *New England Journal of Medicine, 381*(5), 455–464. https://doi.org/10.1056/NEJMra1706910
29. [23] Rossidis, A. C., Stratigis, J. D., Chadwick, A. C., Hartman, H. A., Ahn, N. J., Li, H., Singh, K., Coons, B. E., Li, L., Lv, W., Zoltick, P. W., Alapati, D., Zacharias, W., Jain, R., Morrisey, E. E., Musunuru, K., & Peranteau, W. H. (2018). In utero CRISPR-mediated therapeutic editing of metabolic genes. *Nature Medicine, 24*(10), 1513–1518. https://doi.org/10.1038/s41591-018-0184-6
30. [24] Coons, B., & Peranteau, W. H. (2021). Prenatal gene therapy for metabolic disorders. *Clinical Obstetrics and Gynecology, 64*(4), 904–916. https://doi.org/10.1097/GRF.0000000000000662
31. [25] Bose, S. K., Kennedy, K., & Peranteau, W. H. (2023). Foetal genome editing. *Current Opinion in Obstetrics and Gynecology, 35*(2), 134–139. https://doi.org/10.1097/GCO.0000000000000854
32. [26] Bose, S. K., White, B. M., Kashyap, M. V., et al. (2021). In utero adenine base editing corrects multi-organ pathology in a lethal lysosomal storage disease. *Nature Communications, 12*, 4291. https://doi.org/10.1038/s41467-021-24443-8
33. [27] Słyk, Ż., Stachowiak, N., & Małecki, M. (2024). Recombinant adeno-associated virus vectors for gene therapy of the central nervous system: Delivery routes and clinical aspects. *Biomedicines, 12*(7), 1523. https://doi.org/10.3390/biomedicines12071523
34. [28] Levers, T. E., Edgar, J. M., & Price, D. J. (2001). The fates of cells generated at the end of neurogenesis in developing mouse cortex. *Journal of Neurobiology, 48*(4), 265–277. https://doi.org/10.1002/neu.1056
35. [29] Zorn, A. M. (2008). Liver development. In *StemBook*. NIH/National Center for Biotechnology Information. https://www.ncbi.nlm.nih.gov/books/NBK52644/

36. [30] Telley, L., Agirman, G., Prados, J., Amberg, N., Fièvre, S., Oberst, P., … Hippenmeyer, S. (2022). Temporal and sequential transcriptional dynamics define lineage shifts in corticogenesis. *The EMBO Journal.* https://doi.org/10.15252/embj.2022111132
37. [31] Lui, J. H., Hansen, D. V., & Kriegstein, A. R. (2011). Progenitor cell diversity in the developing mouse neocortex. *Nature Reviews Neuroscience, 12*(5), 327–338. https://doi.org/10.1038/nrn3049
38. [32] Vasan, L., Moffat, A., Mattar, P., & Schuurmans, C. (2025). Neocortical neurogenesis: A proneural gene perspective. *FEBS Journal, 292*(21), 5580–5610. https://doi.org/10.1111/febs.70158
39. [33] Waddington, S. N., Kramer, M. G., Hernandez-Alcoceba, R., Buckley, S. M. K., Themis, M., Coutelle, C., & Prieto, J. (2005). In utero gene therapy: Current challenges and perspectives. *Molecular Therapy, 12*(1), 9–14. https://doi.org/10.1016/j.ymthe.2005.03.002
40. [34] Ahn, N. J., et al. (2018). Intravenous and intra-amniotic in utero transplantation in the murine fetus. *Developmental Biology, 438*(2), 1–9. https://doi.org/10.1016/j.ydbio.2018.08.011
41. [35] Mattar, C. N. Z., Chew, W. L., & Lai, P. S. (2024). Embryo and fetal gene editing: Technical challenges and progress toward clinical applications. *Molecular Therapy — Methods & Clinical Development, 32*(2), 101229. https://doi.org/10.1016/j.omtm.2024.101229
42. (36) Thompson, C. L., Ng, L., Menon, V., Martinez, S., Lee, C. K., Glattfelder, K., Sunkin, S. M., Henry, A., Lau, C., Dang, C., Garcia-Lopez, R., Martinez-Ferre, A., Pombero, A., Rubenstein, J. L. R., Wakeman, W. B., Hohmann, J., Dee, N., Sodt, A. J., Young, R., … Jones, A. R. (2014). A high-resolution spatiotemporal atlas of gene expression of the developing mouse brain. *Neuron*, 83(2), 309–323. https://doi.org/10.1016/j.neuron.2014.05.033
43. [37] Jang, M. J., Coughlin, G. M., Jackson, C. R., Chen, X., Chuapoco, M. R., Vendemiatti, J. L., Wang, A. Z., & Gradinaru, V. (2023). Spatial transcriptomics for profiling the tropism of viral vectors in tissues. *Nature Biotechnology,* 41, 1272–1286. https://doi.org/10.1038/s41587-022-01648-w
44. [38] Goertsen, D., Flytzanis, N. C., Goeden, N., Chuapoco, M. R., … Gradinaru, V. (2022). AAV capsid variants with brain-wide transgene expression and decreased liver targeting after intravenous delivery in mouse and marmoset. Nature Neuroscience, 25(1), 106–115. https://doi.org/10.1038/s41593-021-00969-4
45. [39] Chen, X., Wolfe, D. A., Bindu, D. S., Zhang, M., Taskin, N., … Gradinaru, V. (2023). Functional gene delivery to and across brain vasculature of systemic AAVs with endothelial-specific tropism in rodents and broad tropism in primates. Nature Communications, 14(1), 3345. https://doi.org/10.1038/s41467-023-38582-7

46. [40] DeLeve, L. D., Wang, X., & Guo, Y. (2019). Functions and the emerging role of the foetal liver in regenerative medicine. *Journal of Clinical Medicine, 8*(6), 101229. https://doi.org/10.3390/jcm8061012297
47. [41] Zorn, A. M., & Wells, J. M. (2012). Histology atlas of the developing mouse hepatobiliary hemolymphatic vascular system with emphasis on embryonic days 11.5–18.5 and early postnatal development. *Developmental Biology.* https://doi.org/10.1177/0192623316630836
48. [42] Mattar, C. N., Wong, A. M., Hoefer, K., Alonso-Ferrero, M. E., Buckley, S. M., Howe, S. J., Cooper, J. D., Waddington, S. N., & Chan, J. K. Y., Rahim, A. A. (2015). Systemic gene delivery following intravenous administration of AAV9 to fetal and neonatal mice and late-gestation nonhuman primates. *FASEB Journal, 29*(9), 3876–3888. https://doi.org/10.1096/fj.14-269092
49. [43] Kawabata, H., Konno, A., Matsuzaki, Y., Sato, Y., Kawachi, M., Aoki, R., Tsutsumi, S., Togai, S., Kobayashi, R., Horii, T., Hatada, I., & Hirai, H. (2024). Improving cell-specific recombination using AAV vectors in the murine CNS by capsid and expression cassette optimization. *Molecular Therapy — Methods & Clinical Development, 32*(1), 101185. https://doi.org/10.1016/j.omtm.2024.101185
50. [44] Lang, J. F., Toulmin, S. A., Brida, K. L., Eisenlohr, L. C., & Davidson, B. L. (2019). Standard screening methods underreport AAV-mediated transduction and gene editing. *Nature Communications, 10*, 3415. https://doi.org/10.1038/s41467-019-11321-7
51. [45] Frotscher, M., Chai, X., Bock, H. H., Haas, C. A., Förster, E., & Zhao, S. (2009). Role of Reelin in the development and maintenance of cortical lamination. *Journal of Neural Transmission (Vienna), 116*(11), 1451–1455. https://doi.org/10.1007/s00702-009-0228-7
52. [46] Tissir, F., & Goffinet, A. (2003). Reelin and brain development. *Nature Reviews Neuroscience, 4*, 496–505. https://doi.org/10.1038/nrn1113
53. [47] Hamad, M. I. K., Jbara, A., Rabaya, O., Petrova, P., Daoud, S., Melliti, N., Meseke, M., Lutz, D., Petrasch-Parwez, E., Schwitalla, J. C., Mark, M. D., Herlitze, S., Reiss, G., Herz, J., & Förster, E. (2021). Reelin signaling modulates GABAB receptor function in the neocortex. *Journal of Neurochemistry, 156*(5), 589–603. https://doi.org/10.1111/jnc.14990
54. [48] Nishiyama, J., Mikuni, T., & Yasuda, R. (2017). Virus-mediated genome editing via homology-directed repair in mitotic and postmitotic cells in mammalian brain. *Neuron, 96*(4), 755–768.e5. https://doi.org/10.1016/j.neuron.2017.10.004
55. [49] Chan, K., Jang, M., Yoo, B., et al. (2017). Engineered AAVs for efficient noninvasive gene delivery to the central and peripheral nervous systems. *Nature Neuroscience, 20*, 1172–1179. https://doi.org/10.1038/nn.4593
56. [50] Wang, J. C., Ding, S. H., He, Z. H., Huang, J. L., Weng, W. J., Gao, Y. W., Jiang, J. Y., Lin, Y., & Feng, J. F. (2025). Dynein-regulated brain transduction of AAV.CAP-B10 via cerebral lateral ventricle enhances hippocampal function after traumatic brain injury through Ngf gene delivery in mice. *Experimental Neurology, 391*, 115285. https://doi.org/10.1016/j.expneurol.2025.115285

57. [51] Velazquez-Rivera, E., Dey, O., Kim, N. S., Cao, W., Ye, Q., Gao, P., Thai, A., Nguyen, J. K., Zhang, H., Ting, J. T., Gopi, M., Ren, B., Holmes, T. C., & Xu, X. (2025). Specific targeting of brain endothelial cells using enhancer AAV vectors. *Neuron, 113*(10), 1562–1578.e6. https://doi.org/10.1016/j.neuron.2025.03.031
58. [52] Dotiwala, A. K., McCausland, C., & Samra, N. S. (2025). Anatomy, head and neck: Blood brain barrier. In *StatPearls* [Internet]. Treasure Island (FL): StatPearls Publishing. https://www.ncbi.nlm.nih.gov/books/NBK519556/]
59. [53] Madisen, L., Zwingman, T., Sunkin, S. et al. A robust and high-throughput Cre reporting and characterization system for the whole mouse brain. Nat Neurosci 13, 133–140 (2010). https://doi.org/10.1038/nn.2467
60. [54] Frotscher M, Chai X, Bock HH, Haas CA, Förster E, Zhao S. Role of Reelin in the development and maintenance of cortical lamination. J Neural Transm (Vienna). 2009 Nov;116(11):1451-5. doi: 10.1007/s00702-009-0228-7. Epub 2009 Apr 25. PMID: 19396394.
61. [55] Badea, A., Nicholls, P. J., Johnson, G. A., & Wetsel, W. C. (2007). Neuroanatomical phenotypes in the reeler mouse. NeuroImage 34(4):1363–1374. https://doi.org/10.1016/j.neuroimage.2006.09.053
62. [56] Li, G., Yang, X., Luo, X., Wu, Z., & Yang, H. (2023). Modulation of cell cycle increases CRISPR-mediated homology-directed DNA repair. *Cell & Bioscience, 13*(1), 215. https://doi.org/10.1186/s13578-023-01159-4
63. [57] Lomova, A., Clark, D. N., Campo-Fernandez, B., Flores-Bjurström, C., Kaufman, M. L., Fitz-Gibbon, S., Wang, X., Miyahira, E. Y., Brown, D., DeWitt, M. A., Corn, J. E., Hollis, R. P., Romero, Z., & Kohn, D. B. (2019). Improving gene editing outcomes in human hematopoietic stem and progenitor cells by temporal control of DNA repair. *Stem Cells, 37*(2), 284–294. https://doi.org/10.1002/stem.2935
64. [58] Russ, J. B., Agarwal, S., Venkatesan, C., Scelsa, B., Vollmer, B., Tarui, T., Pardo, A. C., Lemmon, M. E., Mulkey, S. B., Hart, A. R., Nagaraj, U. D., Kuller, J. A., Whitehead, M. T., Cohen, J. L., Gebb, J. S., Glenn, O. A., Norton, M. E., & Gano, D. (2025). Fetal malformations of cortical development: review and clinical guidance. Brain, 148(6), 1888–1903. https://doi.org/10.1093/brain/awaf094
65. [59] Patten, B. M. (Ed.). (2019). Embryology, weeks 6–8. In *Neurodevelopmental biology*. NCBI Bookshelf. https://www.ncbi.nlm.nih.gov/books/NBK563181/
66. [60] Rakic, P., & Zecevic, N. (2015). Physical biology of human brain development. *Frontiers in Cellular Neuroscience, 9*, 257. https://doi.org/10.3389/fncel.2015.00257
67. [61] Ni, W., Cai, Z., & Huang, T. (2021). Comparative neurogenesis timing in mammalian cortex: Insights into developmental scaling. *Frontiers in Cell and Developmental Biology, 9*, 676911. https://doi.org/10.3389/fcell.2021.676911
68. [62] Degl'Innocenti, E., & Dell'Anno, M. T. (2023). Human and mouse cortical astrocytes: A comparative view from development to morphological and functional characterization. *Frontiers in Neuroanatomy, 17*, 1130729. https://doi.org/10.3389/fnana.2023.1130729